

ANKARA YILDIRIM BEYAZIT UNIVERSITY

GRADUATE SCHOOL OF NATURAL AND APPLIED SCIENCES



**FIRST AND SECOND LAW ANALYSIS OF COMPACT HEAT
EXCHANGERS USED FOR INTERCOOLING PURPOSES**

M.Sc. Thesis by

Ahmet Yasin SEDEF

Department of Mechanical Engineering

January, 2017

ANKARA

**FIRST AND SECOND LAW ANALYSIS OF COMPACT
HEAT EXCHANGERS USED FOR INTERCOOLING
PURPOSES**

A Thesis Submitted to

The Graduate School of Natural and Applied Sciences of

Ankara Yıldırım Beyazıt University

**In Partial Fulfillment of the Requirements for the Degree of Master of Science
in Mechanical Engineering, Department of Mechanical Engineering**

by

Ahmet Yasin SEDEF

January, 2017

ANKARA

M.Sc. THESIS EXAMINATION RESULT FORM

We have read the thesis entitled “**FIRST AND SECOND LAW ANALYSIS OF COMPACT HEAT EXCHANGERS USED FOR INTERCOOLING PURPOSES**” completed by **AHMET YASİN SEDEF** under the supervision of **ASSIST. PROF. DR. KEMAL BİLEN** and we certify that in our opinion it is fully adequate, in scope and in quality, as a thesis for the degree of Master of Science.

Assist. Prof. Dr. Kemal BİLEN

Supervisor

Assoc. Prof. Dr. Malik M. NAUMAN

Jury Member

Prof. Dr. Atilla BIYIKOĞLU

Jury Member

Prof. Dr. Fatih V. ÇELEBİ

Director

Graduate School of Natural and Applied Sciences

ETHICAL DECLARATION

I hereby declare that, in this thesis which has been prepared in accordance with the Thesis Writing Manual of Graduate School of Natural and Applied Sciences,

- All data, information and documents are obtained in the framework of academic and ethical rules,
- All information, documents and assessments are presented in accordance with scientific ethics and morals,
- All the materials that have been utilized are fully cited and referenced,
- No change has been made on the utilized materials,
- All the works presented are original,

and in any contrary case of above statements, I accept to renounce all my legal rights.

ACKNOWLEDGMENTS

Firstly, I would like to express my sincere gratitude to my supervisor, Assist. Prof. Dr. Kemal BİLEN for his tremendous support and motivation during my study. His immense knowledge and precious recommendations constituted the milestones of this study. His guidance assisted me all the time of my research and while writing this thesis.

I would like to thank Prof. Dr. Veli ÇELİK for his understanding and endless support. He always motivated me during my hard times and his advices helped me a lot to overcome problems.

I also would like thank Assoc. Prof. Dr. Malik Muhammed NAUMAN and Prof. Dr. Atilla BIYIKOĞLU for their valuable contributions and constructive criticisms during my thesis defense examination.

I am grateful to my friend Ömer YILDIRIM for his superior contribution and great effort while preparing the computer program for my thesis. Also my dearest friends Hasan Ersel GÜREL and Meltem YAKTUBAY provided me enormous support during my study and always trusted me. I am very fortunate to have such friends.

Finally, I must express my profound appreciations to my family for providing me emotional support, loving care and continuous encouragement throughout my years of study and through the period of writing this thesis. This accomplishment would not have been possible without them. Thank You.

2017, 12 January

Ahmet Yasin SEDEF

FIRST AND SECOND LAW ANALYSIS OF COMPACT HEAT EXCHANGERS USED FOR INTERCOOLING PURPOSES

ABSTRACT

Intercooling is a process that is employed in turbocharged engines to cool the charge air. This cooling enables to feed more air into the cylinders and decreases the operating temperatures of the engine. Intercoolers -kind of compact heat exchangers- are used to carry out this process. Depending on the required thermal-hydraulic performance, intercoolers can be designed using different fin types.

In this study, the fin types that are utilized in the design of intercoolers are theoretically examined using the first and second law of thermodynamics. For this purpose, various intercooler configurations are established with five different fin geometries, namely plain fins, louvered fins, offset strip fins, wavy fins and perforated fins. Then, sizing and rating procedures are applied on these configurations. In sizing procedure, the dimensions of the intercooler configurations are determined. In rating procedure, heat transfer, pressure drop and second law performances of the configurations are computed. The obtained results are tabulated and compared with each other.

It is found that offset strip fins provide very good heat transfer performances whereas plain fins enable least pressure drops in the fluid pressures. In second law analysis the following outcome is attained; since the configurations in this study have unbalanced flow, eliminating entropy generation or exergy destruction is not possible even with an infinite surface area and zero pressure drops.

Keywords: Turbocharging, intercooling, intercoolers, compact heat exchangers, plate-fin heat exchangers, heat transfer, pressure drop, second law analysis.

ARA SOĞUTMA AMAÇLI KULLANILAN KOMPAKT ISI DEĞİŞTİRİCİLERİNİN BİRİNCİ VE İKİNCİ YASA ANALİZLERİ

ÖZ

Aşırı doldurmalı motorlarda, dolgu havasının sıcaklığını düşürmek amacıyla ara soğutma işlemi uygulanır. Yapılan soğutma ile motora beslenen hava miktarında artış, motordaki genel sıcaklık seviyesinde ise azalma sağlanır. Bu soğutma işlemi, bir kompakt ısı değıştircisi olan ara soğutucu ile gerçekleştirilir. İhtiyaç duyulan termal-hidrolik performansa bağılı olarak ara soğutucular, farklı kanatçık tipleri kullanılarak tasarlanabilir.

Yapılan bu çalışmada; ara soğutucu tasarımında kullanılan kanatçık tipleri, birinci ve ikinci yasa analizleri vasıtasıyla teorik olarak incelenmiştir. Bu kapsamda; düz kanatçık, panjurlu kanatçık, kaydırılmış şerit kanatçık, dalgalı kanatçık ve delikli kanatçık olmak üzere beş kanatçık tipi kullanılarak farklı ara soğutucu yapıları kurgulanmıştır. Daha sonra bu yapılara boyutlandırma ve performans değerlendirme işlemleri uygulanmıştır. Boyutlandırma işlemi ile ara soğutucu yapılarının ebatları bulunurken, performans değerlendirme işlemi ile yapıların ısı geçişi, basınç düşümü ve ikinci yasa performansı hesaplanmıştır. Elde edilen sonuçlar tablolar halinde verilmiş ve birbirleriyle kıyaslanmıştır.

Sonuçlar, kaydırılmış şerit kanatçık tipinin kullanılması ile ısılı açıdan iyi bir performans elde edilebileceğini, düz kanatçık tipinin kullanılması ile de akışkanların en az miktarda basınç düşüşüne maruz kalacağını göstermiştir. İkinci yasa analizleri ise; bu çalışmadaki ara soğutucuların dengeli akışa sahip olmaması nedeniyle, sonsuz büyüklükteki bir yüzey alanı ve sıfır basınç kaybıyla bile ara soğutucuda entropi üretiminin ya da ekserji yıkımının tamamen yok edilemeyeceğini göstermiştir.

Anahtar Kelimeler: Aşırı doldurma, ara soğutma, ara soğutucular, kompakt ısı değıştircileri, plakalı-kanatlı ısı değıştircileri, ısı geçişi, basınç düşümü, ikinci yasa analizi.

CONTENTS

M.Sc. THESIS EXAMINATION RESULT FORM	ii
ETHICAL DECLARATION	iii
ACKNOWLEDGMENTS	iv
ABSTRACT	v
ÖZ.....	vi
NOMENCLATURE	ix
LIST OF TABLES	xii
LIST OF FIGURES	xiii
CHAPTER 1 - INTRODUCTION.....	1
1.1 A General View of Internal Combustion Engines	2
1.1.1 Engine Classifications	2
1.1.2 Engine Operating Cycles	3
1.2 Supercharging of Internal Combustion Engines.....	5
1.2.1 Mechanical Supercharging	8
1.2.2 Turbocharging.....	8
1.2.3 Pressure Wave Supercharging.....	9
1.3 Intercooling in Internal Combustion Engines	9
1.4 A General View of Heat Exchangers	11
1.4.1 Heat Exchanger Classifications	12
1.4.2 Compact Heat Exchangers.....	14
1.5 Aim of the Study.....	16
1.6 Review of Related Works	17
CHAPTER 2 - BASICS OF INTERCOOLERS.....	21
2.1 General Design Considerations of Intercoolers.....	21
2.2 Theory of Intercoolers	22
2.2.1 Thermal Design	22
2.2.2 Pressure Drop Analysis.....	27
2.2.3 Second Law Analysis.....	30
2.3 Some Additional Considerations for Thermal Design.....	35
2.3.1 Influence of Temperature-Dependent Fluid Properties	35
2.3.2 Longitudinal Heat Conduction Effects	36

2.3.3 Determination of Plate-fin Efficiency	38
CHAPTER 3 - DESIGN PROCEDURES OF INTERCOOLERS	42
3.1 Some Selected Surface Types and Their Characteristics.....	42
3.1.1 Colburn Factor and Fanning Friction Factor	43
3.2 Operating Conditions of Intercooler.....	44
3.3. Rating Problem.....	47
3.4 Sizing Problem	51
CHAPTER 4 - RESULTS.....	55
4.1 Sizing Results	56
4.2 Rating Results.....	59
4.2.1 Comparison in terms of Heat Transfer and Pressure Drop Performance.	59
4.2.2 Comparison in terms of Second Law of Thermodynamics	62
4.2.3 Variation of Performance Parameters with Mass Flow Rate	66
4.3 Intercooler and Engine Performance Results	71
CHAPTER 5 - DISCUSSION AND CONCLUSION.....	76
REFERENCES.....	80
APPENDICES	84
Appendix A – Surface Characteristics of Fins.....	85
Appendix B – j and f Factor Equations and Reynolds Number Ranges	86
Appendix C – Thermophysical Properties of Air	89
Appendix D – K_c and K_e Coefficients	90
CURRICULUM VITAE	91

NOMENCLATURE

Roman Letter Symbols

A	Heat transfer area, m^2
A_f	Fin surface area, m^2
A_{fr}	Frontal area, m^2
A_k	Cross-sectional area for longitudinal heat conduction, m^2
A_o	Free flow area, m^2
A_w	Wall conduction area, m^2
b	Plate spacing, mm
C	Heat capacity rate, kW/K
C^*	Heat capacity rate ratio
c_p	Specific heat at constant pressure, kJ/(kg·K)
D_h	Hydraulic diameter, mm
D	Destroyed exergy, W
f	Fanning friction factor
G	Core mass velocity, kg/($m^2 \cdot s$)
h	Convection heat transfer coefficient, W/($m^2 \cdot K$), specific enthalpy, kJ/kg
I	Irreversibility, W
I^*	Non-dimensional exergy destruction
j	Colburn factor
k	Thermal conductivity, W/($m \cdot K$), specific heat ratio
K_c	Entrance (contraction) pressure loss coefficient
K_e	Exit (expansion) pressure loss coefficient
l	Length of the fin, mm
L	Flow length, mm
L_f	Fin flow length, mm
\dot{m}	Mass flow rate, kg/s
n	Number of revolutions of the crankshaft for one thermodynamic cycle, rev/cycle
N	Engine speed, rpm
N_p	Number of passages
N_s	Entropy generation number (by Bejan)

$N_{s,1}$	Entropy generation number (by Hesselgreaves)
$N_{s,a}$	Augmentation entropy generation number
Nu	Nusselt number
ntu	Number of heat transfer units based on the fluid side
NTU	Number of heat transfer units of a heat exchanger
q	Heat transfer rate, W
q''	Heat flux, W/m ²
P	Absolute pressure, kPa
Pr	Prandtl number
R	Specific gas constant, kJ/(kg·K)
R_w	Wall thermal resistance, K/W
Re	Reynolds number
s	Specific entropy, kJ/(kg·K)
\dot{S}_{gen}	Total entropy generation rate, kW/K
$\dot{S}_{gen,\Delta T}$	Entropy generation rate due to finite temperature difference, kW/K
$\dot{S}_{gen,\Delta P}$	Entropy generation rate due to fluid friction, kW/K
St	Stanton number
T	Absolute temperature, K
U	Overall heat transfer coefficient, W/(m ² ·K)
V	Velocity, m/s, volume, m ³
V_d	Total displacement volume, L

Greek Letter Symbols

α	Ratio of heat transfer area of one side to total heat exchanger volume, m ² /m ³
β	Surface area density, m ² /m ³
δ	Thickness, mm
Δ	Difference
ε	Exchanger effectiveness
ε_R	Rational (second law) effectiveness
η_f	Efficiency of fin
η_o	Efficiency of extended (or total) surface
η_s	Second law efficiency
λ	Longitudinal wall heat conduction parameter

μ	Dynamic viscosity of fluid, N·s/m ²
ν	Specific volume of fluid, m ³ /kg
ρ	Density of fluid, kg/m ³
σ	Ratio of free-flow area to frontal area
τ_w	Surface (wall) shear stress, kg/(m·s ²)
ψ	Flow exergy, kJ/kg

Subscripts

c	Cold fluid
f	Fin
h	Hot fluid
i	Inlet
m	Mean
max	Maximum
min	Minimum
o	Outlet
st	Stack
w	Wall
0	Reference (temperature or pressure)
1, 2	Any flow side of the heat exchanger (hot or cold side)

Acronyms

BDC	Bottom Dead Center
CI	Compression-ignition
ICE	Internal Combustion Engine
LHC	Longitudinal Heat Conduction
LMTD	Logarithmic Mean Temperature Difference
SI	Spark-ignition
TDC	Top Dead Center

LIST OF TABLES

Table 2.1 Exponents of (T_w/T_m)	36
Table 3.1 Technical specifications of Ford Cargo TCI engine	46
Table 4.1 Sizing results of intercooler configurations.....	57
Table 4.2 Thermal-hydraulic performance results of intercooler configurations.....	60
Table 4.3 Second law performance results of intercooler configurations.	63
Table 4.4 Charge air density and temperatures in the cycle for different engine operation types.	72
Table A.1 Surface characteristics of fins.....	85
Table B.1 j factor equations for fin types.	86
Table B.2 f factor equations for fin types.....	87
Table B.3 Reynolds number ranges for j and f factor equations	88
Table C.1 Thermophysical properties of air at one atmospheric pressure	89

LIST OF FIGURES

Figure 1.1 Four-stroke SI engine cycle	4
Figure 1.2 A two-stroke SI engine	5
Figure 1.3 Supercharging and turbocharging configurations.....	7
Figure 1.4 Types of charge air cooling systems.....	11
Figure 1.5 Schematic diagram of a plate-fin heat exchanger	15
Figure 1.6 Various fin geometries for plate-fin heat exchangers.....	16
Figure 2.1 Depiction of heat transfer in a counterflow heat exchanger	24
Figure 2.2 Pressure drop components in a plate-fin exchanger flow passage.....	28
Figure 2.3 Straight, thin fin with uniform rectangular cross-section	40
Figure 2.4 (a) Plain rectangular fin and (b) plain triangular fin	41
Figure 3.1 Charge air flow in a turbocharged and intercooled engine	45
Figure 4.1 The change of effectiveness with respect to hot side mass flow rate.	67
Figure 4.2 The change of hot side pressure drop with respect to hot side mass flow rate.....	68
Figure 4.3 The change of hot side outlet density with respect to hot side mass flow rate.....	69
Figure 4.4 The change of total entropy generation rate with respect to hot side mass flow rate	69
Figure 4.5 The change of normalized entropy generation rate with respect to hot side mass flow rate	70
Figure 4.6 The change of second law efficiency with respect to hot side mass flow rate.....	71
Figure 4.7 P-v diagram of an air-standard dual cycle	72
Figure 4.8 Effect of charge cooling on inlet air density.....	74
Figure 4.9 Effect of pressure drop on inlet air density.....	75
Figure D.1 Entrance and exit pressure loss coefficients	90

CHAPTER 1

INTRODUCTION

Internal combustion engines (ICE) have found wide application in today's world, especially in the land, sea, and air transportation sectors and power generation fields. ICEs are highly preferred because of their simplicity, durability and high power to weight ratios. On the other hand, their most critical and vital problem is the emissions generated by the engine. These emissions pollute the environment and threaten human health. Therefore the allowable emission levels for the engines are decreased day by day. More efficient and low emissions power generation has become very crucial.

Supercharging the ICEs, that is providing compressed air to the engine cylinders, is one way of increasing the engine efficiency and decreasing the emissions. It is a process of pressurizing the air (so increasing density of the air) before entry to cylinders. Therefore more fuel can be fed and more power can be generated efficiently without changing the engine size. Supercharging process has many advantages but it generally requires some additional modifications to the engine. Increasing the pressure also increases the temperature of intake air by compressive heating which in turn elevates the temperatures throughout the entire engine operating cycle. This condition overshadows the positive effect of supercharging. In order to eliminate it, a process often called intercooling (or aftercooling, charge air cooling) is performed in supercharged engines by means of intercoolers -kind of compact heat exchangers. This intercooling process also further increases the density of charge air which is very desirable.

When intercoolers are utilized, the compressed air leaving the supercharger is directed to the intercooler and cooled using a fluid. Here the important point is that; intercooler must provide necessary amount of cooling to the charge air without dropping its pressure much. If not so, the advantages gained by supercharging are diminished and practicality of intercooling process becomes questionable.

In this chapter, firstly a brief explanation of internal combustion engines is introduced. Then, supercharging and intercooling applications employed in internal combustion engines are described in details. Since intercoolers are essentially heat exchangers, heat exchanger classifications, and the position of intercoolers in given classifications are mentioned. Last, the aim of this study and related works in the literature are presented.

1.1 A General View of Internal Combustion Engines

Internal combustion engines date back to 1876 when Otto first created the spark-ignition engine and 1892 when Diesel developed the compression-ignition engine. Since then, these engines have been continuously improved as new technologies or advancements have become available. The demand for new types of engines and environmental constraints are the main causes of that ongoing development. Today these engines play a dominant role in fields of power, propulsion and energy [1].

The purpose of internal combustion engines is the production of mechanical power from the chemical energy of the fuel. This energy is released by burning or oxidizing the fuel inside the engine. Because this energy supplied to the engine parts is created *inside* the engine, it is called *internal* combustion engine (ICE).

ICEs which are the subjects of this study are spark-ignition (SI) or gasoline engines (although other fuels can be used) and compression-ignition (CI) or diesel engines. Gas turbines are also internal combustion engines by this definition, yet, customarily; the term is only used for SI and CI engines.

Because of their simplicity, durability and high power to weight ratio, SI and CI engines have found wide application in transportation sectors (land, sea and air) and power generation fields [1].

1.1.1 Engine Classifications

There are many different types of internal combustion engines. They can be classified by [1]:

1. *Application.* Automobile, truck, locomotive, light aircraft, marine, portable power system, power generation.
2. *Basic engine design.* Reciprocating engines, rotary engines.
3. *Working cycle.* Four-stroke cycle, two-stroke cycle.
4. *Valve or port design and location.* Overhead (or I-head) valves, underhead (or L-head) valves, rotary valves, cross-scavenged porting, loop-scavenged porting, through- or uniflow-scavenged.
5. *Fuel.* Gasoline (or petrol), fuel oil (or diesel fuel), natural gas, liquid petroleum gas, alcohols (methanol, ethanol), hydrogen, dual fuel.
6. *Method of mixture preparation.* Carburetion, fuel injection into the intake ports or intake manifold, fuel injection into the engine cylinder.
7. *Method of ignition.* Spark ignition, compression ignition.
8. *Method of air intake process.* Naturally aspirated, supercharged, turbocharged [2].
9. *Combustion chamber design.* Open chamber, divided chamber.
10. *Method of load control.* Throttling of fuel and air flow together so mixture composition is essentially unchanged, control of fuel alone, a combination of these.
11. *Method of cooling.* Water cooled, air cooled, uncooled (other than by natural convection and radiation)
12. *Position and number of cylinders of reciprocating engines.* Single cylinder engine, in-line engine, V engine, opposed cylinder engine, W engine, opposed piston engine, radial engine [2].

1.1.2 Engine Operating Cycles

Most internal combustion engines, both SI and CI, operate on either a four-stroke cycle or a two-stroke cycle. These cycles are quite standard for all engines. Only slight variations may be found in separate designs [2].

In a four-stroke engine, piston in each cylinder has four strokes; intake, compression, power and exhaust strokes, to complete its cycle. This corresponds to two revolutions of the crankshaft.

For an SI engine, in intake stroke, the piston moves from top-dead-center (TDC) to bottom-dead-center (BDC) and draws fresh air-fuel mixture through the open intake valve into the cylinder. In compression stroke, the piston moves from BDC to TDC to compress that mixture. The temperature and pressure inside the cylinder is increased to a certain value and the mixture is ignited by a spark plug to initiate combustion toward the end of the stroke. The combustion ideally occurs at constant volume. In power stroke, the high temperature and pressure gas expands and moves the piston to the BDC position. As the piston approaches BDC, the exhaust valve opens to initiate exhaust process. Finally, in exhaust stroke the piston moves from BDC to TDC to sweep out the burned gases. A schematic diagram explaining the entire cycle is given in Figure 1.1.

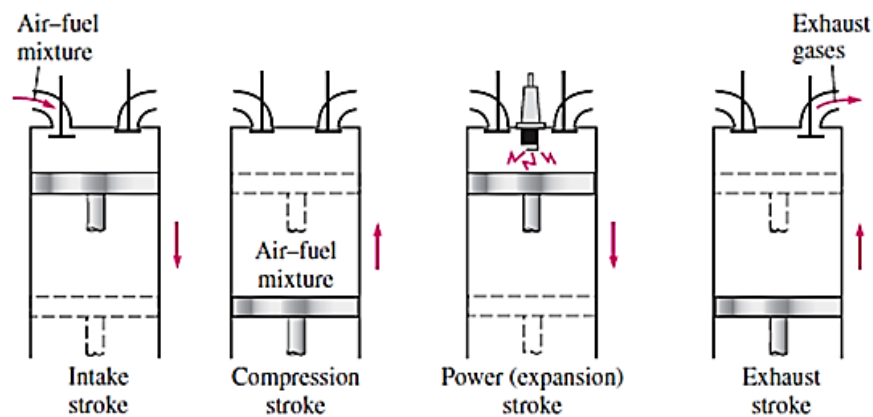


Figure 1.1 Four-stroke SI engine cycle [Modified from 3].

The four-stroke CI or diesel engine goes through the almost same steps with SI engine. Slight differences occur in the cycle. The most important difference is that in CI engine only air is inducted into the cylinder during the intake stroke and combustion is initiated not by a spark plug but injection of fuel over the air. Self-ignition occurs when the fuel meets the air in the cylinder. Combustion proceeds ideally at constant pressure. The remaining steps are identical to the SI engine.

To obtain a higher power output from a given engine size and a simpler valve design, the two-stroke cycle was developed. In two-stroke SI and CI engines, the processes occur with similar manner. However, in these engines one cycle corresponds to one

revolution of the crankshaft. Generally intake and exhaust ports are used instead of valves as seen in Figure 1.2. These ports are opened and closed by the piston motion. A compression stroke and a power stroke complete the cycle [2].

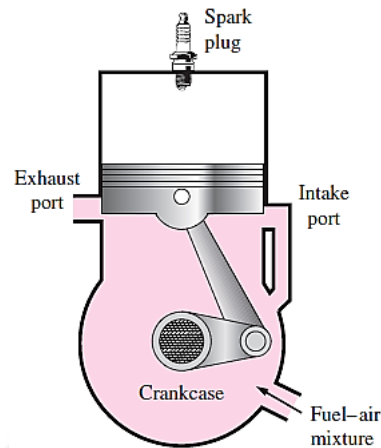


Figure 1.2 A two-stroke SI engine [3].

1.2 Supercharging of Internal Combustion Engines

The maximum power an engine can provide is restricted by the amount of fuel that can be efficiently burned inside the engine cylinders. This in turn, limited by the amount of air that is introduced into these cylinders. If the inducted air (charge air) is compressed to a higher density before entry to cylinders, the maximum power will be increased [1].

In other words, increasing the air density provides more air into the cylinders. This allows proportional increase in the fuel that can be burned and hence raises the potential power output for a given engine. This is the primary purpose of supercharging.

Supercharging process is both applicable to four-stroke and two-stroke engines. However, during supercharging, increasing the pressure of incoming air also increases the temperature of it by compressive heating. This is undesirable for SI engines. If the temperature is higher at the start of the compression stroke, all temperatures in the rest of the cycle will be also higher. This will cause self-ignition

and knocking problems in SI engines [2]. Several parameters can be adjusted to avoid knocking in these engines, yet generally they are not supercharged because of the application difficulties [4]. In CI engines, on the other hand, there is no concern about knocking problems. Supercharged diesel engine output is usually limited by stress levels in critical components. The maximum stress level constrains the maximum cylinder pressure. As charge air pressure is raised, the maximum pressures and thermal loadings will increase nearly in proportion. Therefore, in practice the compression ratio is often reduced in these engines relative to naturally aspirated ones [2]. Supercharging the diesel engines provides high performance and smooth operation.

In two-stroke engines, supercharging is inevitable. Ports are used instead of valves for intake and exhaust processes. These ports are opened and closed with the motion of piston (not by a camshaft). Therefore, in order to clear the cylinder from burned gases and charge it with the fresh air or air-fuel mixture -scavenging process- there should be high-enough pressure of intake. The necessary pressure boost to displace the burned gases can be accomplished by supercharging.

Supercharging which is mainly pressurizing the charge air can be applied to engines in three fundamental methods; Mechanical supercharging, turbocharging and pressure wave supercharging. Figure 1.3 shows typical arrangements of the different supercharging and turbocharging systems.

Most commonly, mechanical supercharger (Fig. 1.3a) or turbocharger (Fig. 1.3b) arrangements are preferred. Combinations of an engine driven compressor and a turbocharger can also be used as in large marine engines (Fig. 1.3c). Two-stage turbocharger is another available method to engines to provide very high pressures (Fig. 1.3d). Turbocompounding which operates with two turbines, one is coupled to compressor and other is directly geared to engine crankshaft, is an alternative method of increasing engine power (Fig. 1.3e). Cooling the compressed air before entry to the cylinders (intercooling) is used to further increase air or mixture density as shown in Fig. 1.3f [1].

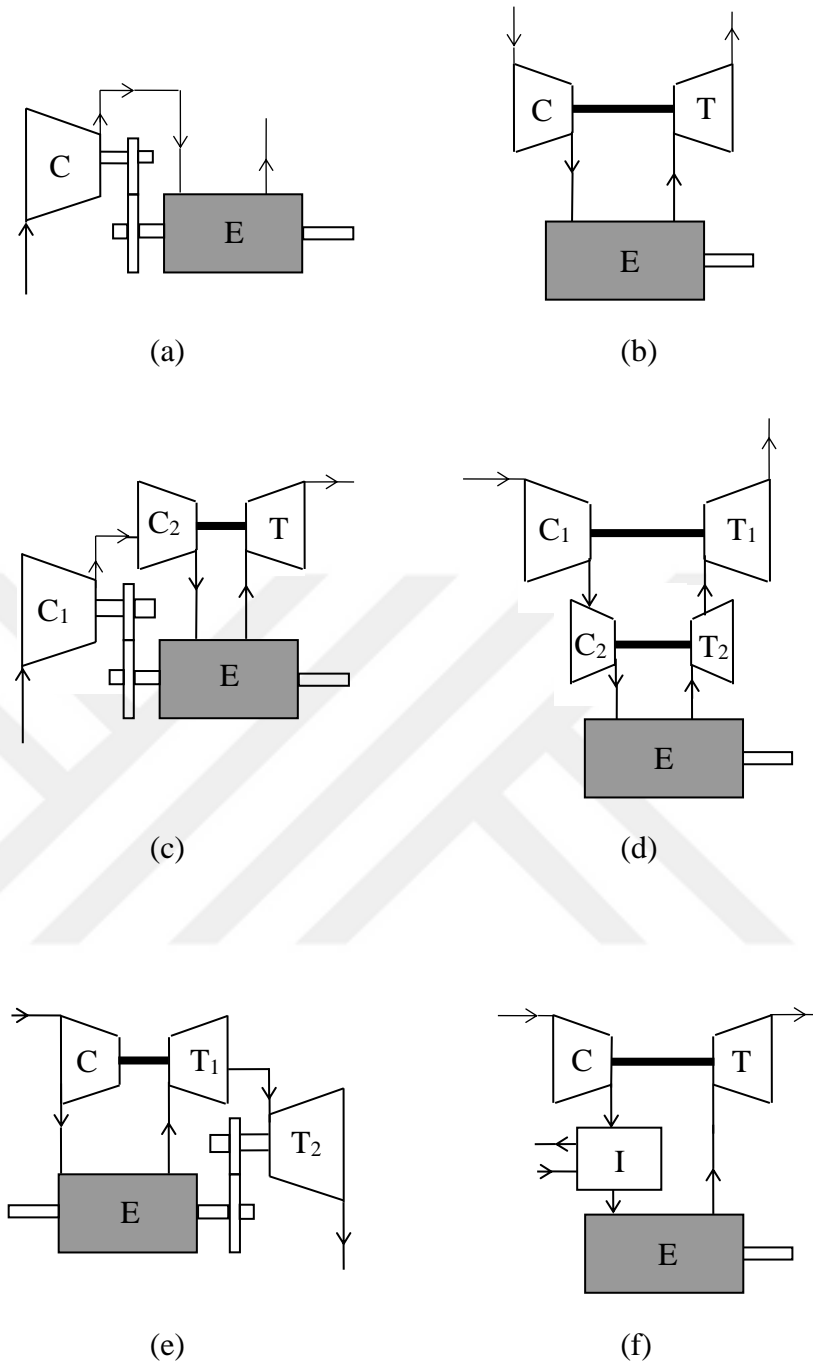


Figure 1.3 Supercharging and turbocharging configurations: (a) mechanical supercharging; (b) turbocharging; (c) engine-driven compressor and turbocharger; (d) two-stage turbocharging; (e) turbocharging with turbocompounding; (f) turbocharger with intercooler. C compressor, E engine, I intercooler and T turbine [1].

1.2.1 Mechanical Supercharging

In this system, a separate compressor usually driven by the engine crankshaft is used to increase the incoming air density. Compressors running at speeds about the same as engine speed are used. A major advantage of this type of supercharging is having very quick response to throttle changes. Being mechanically linked to the crankshaft, any alteration in engine speed is instantly transferred to the compressor [2].

On the other hand, the power to run the compressor is a parasitic (undesired) load on the engine and this creates a drawback for this method. Other disadvantages include higher cost, greater weight and noise [2].

1.2.2 Turbocharging

The second method is combining a compressor with a turbine on a single shaft and using the energy of exhaust gases leaving the cylinders. The exhaust gases passing through turbine rotate its blades and this rotation is transferred to compressor via the common shaft. The compressor then increases the pressure of intake air.

The advantage of this system is none of the engine shaft power output is used to run the compressor and only the waste thermal energy in the exhaust is used. However the existence of the turbine in the exhaust system slightly increases the pressure of exhaust flow and causing a more restricted flow in the ports. This reduces the power output of the engine very slightly but it is compensated and amount of power production can be improved by turbocharging the engine. Also turbocharged engines have lower fuel consumption than the naturally aspirated ones [2].

Turbo lag is a shortcoming of turbochargers and it occurs when there is an abrupt change in throttle position. When the throttle is quickly opened to speed up an automobile, the turbocharger will not react to it as fast as a supercharger will. It takes several engine revolutions to alter exhaust flow rate and to accelerate the turbine rotor. This problem can be solved to high extent by using light ceramic rotors that can both withstand high temperatures and has less inertia of mass. Using smaller intake manifolds also reduce the turbo lag [2].

1.2.3 Pressure Wave Supercharging

It is a type of supercharger technology that harnesses the pressure waves produced by the engine exhaust gas pulses to compress intake mixture. Comprex is an example of a pressure wave supercharging device which utilizes the pressure available in the exhaust gas to compress the inlet mixture by directly contacting the streams in the narrow channels [1].

Energy exchange in this device occurs at the local sound speed which is equal to speed of pressure waves. Therefore the response of the system is fairly quick even at low engine rpms.

Besides these pros, Comprex has several shortcomings. One is that, during the direct contact of intake and exhaust streams there occurs mixing and heat transfer which will lead to increased intake stream temperatures. Mechanical drive complexity and higher cost are other disadvantages of this device [5].

1.3 Intercooling in Internal Combustion Engines

The fundamental reason for supercharging is to increase the power output of an engine without changing its size. This is accomplished by raising the charge air pressure, hence increasing the amount of air inducted into the cylinder and allowing more fuel to be burnt. However, it is not possible to compress air without increasing the temperature of it. This condition downgrades the positive effect of supercharging and partly offsets the benefit of it. The temperature rise decreases the density of air and limits the amount of mass inducted. Therefore while increasing the pressure of the charge air, the temperature rise must be minimized or eliminated. In order to accomplish this and take the full advantage of supercharging, the compressed air is cooled before entry to the cylinders -a process often called intercooling (also called aftercooling or charge air cooling) [6].

In supercharged/turbocharged engines, intercooling is performed by using a heat exchanger named intercooler (also called aftercooler or charge air cooler) and positioned between the compressor and the cylinders. Pressurized air leaving the

compressor is first directed to the intercooler and heat exchange occurs here between air and a cooling fluid. Later, it is fed to the engine cylinders. In this way, the charge air temperature is brought down to a certain value and density of it is further increased just before the intake process. This cooling also decreases the temperature throughout the entire cycle and thus reduces thermal loadings in the engine [6]. Higher compression ratios become available which provides a favorable impact on engine efficiency. In SI engines intercooling also prevents knocking problems [1].

The advantages of charge air cooling are pretty obvious and the technique is commonly used, but it has also some drawbacks. From the fluid dynamics point of view, one problem is that air flow through the intercooler results in a pressure loss. This will deteriorate the density increase obtained by cooling [6]. Weight and size is another issue. The intercooler should be lightweight and as compact as possible. Also the benefits of charge cooling should outweigh the additional cost.

Depending on the application or availability air-to-air or air-to-water cooling systems are used in intercoolers. Various configurations of these systems are given in Figure 1.4.

Air-to-air cooling system (Fig. 1.4a) might be utilized in cases when a source of cooling water is not readily available, and high ambient temperatures restricts the use of local closed cooling system. In this type, the air-to-air intercooler is usually placed in front of the engine coolant radiator. An alternative way of this cooling system (Fig. 1.4b) uses bleed air from the turbocharging system to run the cooling air supply fan. This provides more coolant air flow to the intercooler. Air-to-water cooling systems can use the normal water cooling system of the engine (Fig. 1.4c) or a separate closed water cooling system having its own water-to-air radiator (Fig. 1.4d). The advantage of the first type is the simplicity of installation but the cooling capacity is restricted by the water temperature of the engine cooling system. The latter type does not have such a problem and has a greater potential for cooling [6]. Air-to-water intercooling systems are preferred for marine applications [4].

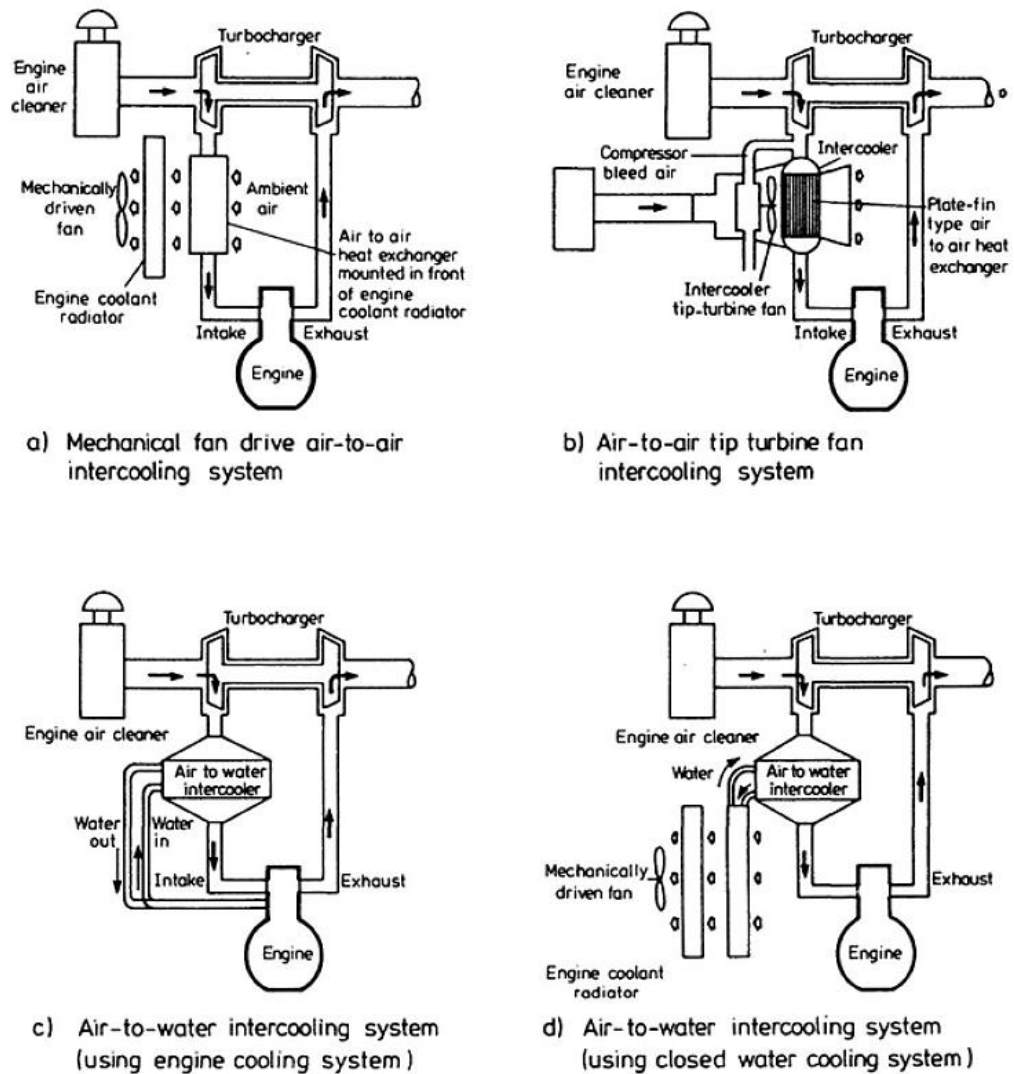


Figure 1.4 Types of charge air cooling systems [6].

1.4 A General View of Heat Exchangers

A heat exchanger is a device that is used to transfer thermal energy between two or more fluids at different temperatures and in thermal contact. Typical applications involve heating or cooling of a fluid stream and evaporation or condensation (phase change) of fluid streams. They have variety of application areas in industry such as process, power, heat recovery, transportation, air-conditioning, refrigeration, and cryogenic industries [7].

1.4.1 Heat Exchanger Classifications

The classification of heat exchangers can be done with many different ways. Main classification types are summarized below.

1.4.1.1 Classification According to Transfer Process

A. Indirect Contact Type Heat Exchangers: In this type of heat exchangers the fluids streams are held apart and heat is transferred via a separating wall.

1. Direct-Transfer Type Exchangers (Recuperators)
2. Storage Type Exchangers (Regenerators)
3. Fluidized-Bed Exchangers

B. Direct Contact Type Heat Exchangers: Two fluid streams are brought into direct contact. Heat exchange occurs between the fluids and then they are separated.

1. Immiscible Fluid Exchangers
2. Gas-Liquid Exchangers
3. Liquid-Vapor Exchangers

1.4.1.2 Classification According to Construction Features

A. Tubular Heat Exchangers

1. Shell-and-Tube Exchangers
2. Double Pipe Exchangers
3. Spiral Tube Exchangers

B. Plate Heat Exchangers

C. Extended Surface Heat Exchangers

1. Plate-Fin Exchangers
2. Tube-Fin Exchangers

D. Regenerative Heat Exchangers

1. Rotary Regenerators
2. Stationary Regenerators

1.4.1.3 Classification According to Flow Arrangements

- A. Single-Pass Heat Exchangers
 - 1. Counterflow Exchangers
 - 2. Parallelflow Exchangers
 - 3. Crossflow Exchangers
 - a) Both fluids unmixed
 - b) One fluid mixed, the other unmixed
 - c) Both fluids mixed
- B. Multipass Heat Exchangers

1.4.1.4 Classification According to Heat Transfer Mechanisms

- A. Single-Phase Convection on Both Sides
- B. Single-Phase Convection on One Side, Two-Phase Convection on Other Side
- C. Two-Phase Convection on Both Sides
- D. Combined Convection and Radiation

1.4.1.5 Classification According to Number of Fluids

- A. Two-Fluid Heat Exchangers
- B. Three-Fluid Heat Exchangers
- C. N-Fluid Heat Exchangers ($N > 3$)

1.4.1.6 Classification According to Fluid Type

- A. Gas-Gas Heat Exchangers
- B. Gas-Liquid Heat Exchangers
- C. Liquid-Liquid Heat Exchangers
- D. Gas-Two Phase Heat Exchangers
- E. Liquid-Two Phase Heat Exchangers

1.4.1.7 Classification According to Surface Compactness

Surface compactness of a heat exchanger is characterized by a parameter called surface area density and denoted by β . It is defined as the ratio of heat transfer

surface area of the given fluid stream side to volume of that side. Sometimes it may be defined with the total volume of the heat exchanger instead of volume of one side as in the case of shell-and-tube exchangers [7].

A. Gas-to-Fluid Heat Exchangers

1. Compact ($\beta \geq 700 \text{ m}^2/\text{m}^3$)
2. Non-compact ($\beta < 700 \text{ m}^2/\text{m}^3$)

B. Liquid-to-Liquid and Phase-Change Heat Exchangers

1. Compact ($\beta \geq 400 \text{ m}^2/\text{m}^3$)
2. Non-compact ($\beta < 400 \text{ m}^2/\text{m}^3$)

1.4.2 Compact Heat Exchangers

Compact heat exchangers are heat exchangers that have high surface area density to enhance heat transfer effectively. Increasing the heat transfer surface area provides a better heat transfer characteristics and hence improves heat transfer. This enables reduced space, weight and cost [7].

The simplest way to obtain a compact surface is to use small diameter tubes that are closely packed constructing a tube bundle. When the fluid flows over this bundle, it experiences high heat transfer surface per unit volume [8].

Another way is to use secondary surfaces, or fins, on one or both fluid sides. Attaching fins to the outside of circular tubes is an example of this method. It is generally used in gas-to-liquid heat exchangers where fins provide an extended surface on the gas side to compensate relatively low heat transfer coefficient of the gas. Tube-fin heat exchanger has this type of arrangement. Fins placed on both fluid sides are preferred in gas-to-gas applications. In this case the heat exchanger is built up as a sandwich of flat plates bonded each other with fins. The fluids flow through the narrow gaps formed by the consecutive pairs of plates. A heat exchanger with such an arrangement is called plate-fin heat exchanger [8]. Figure 1.5 shows an example of this type of exchanger.

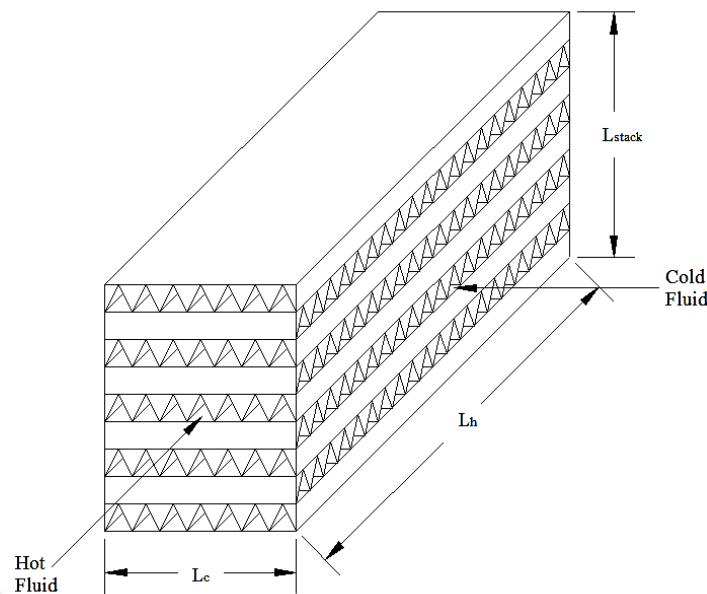


Figure 1.5 Schematic diagram of a plate-fin heat exchanger [4].

1.4.2.1 Plate-fin Heat Exchangers

Most suitable form of heat exchangers for gas-to-gas flow is plate-fin heat exchangers. Having fins on both sides compensate the low heat transfer coefficient characteristic of gases and provide improved heat transfer [8]. The fins attached to the plates are corrugated and commonly have triangular (see Figure 1.5) or rectangular cross-sections [7].

The most functional characteristic of this arrangement is that there is total freedom in selecting the hot and cold side fin surface area, i.e. the compactness of each flow side is independently selected [7]. The surface area densities of 1000 to 2500 m^2/m^3 are common in these arrangements.

These exchangers are categorized further with respect to their fin geometry. Various fin forms are available in the industry. These are (1) plain (i.e. uncut) and straight fins, such as plain triangular and plain rectangular fins, (2) plain but wavy fins (wavy in the fluid flow direction), and (3) interrupted fins, such as offset strip, louvered, perforated and pin fins [7]. Figure 1.6 shows the examples of commonly used fin geometries.

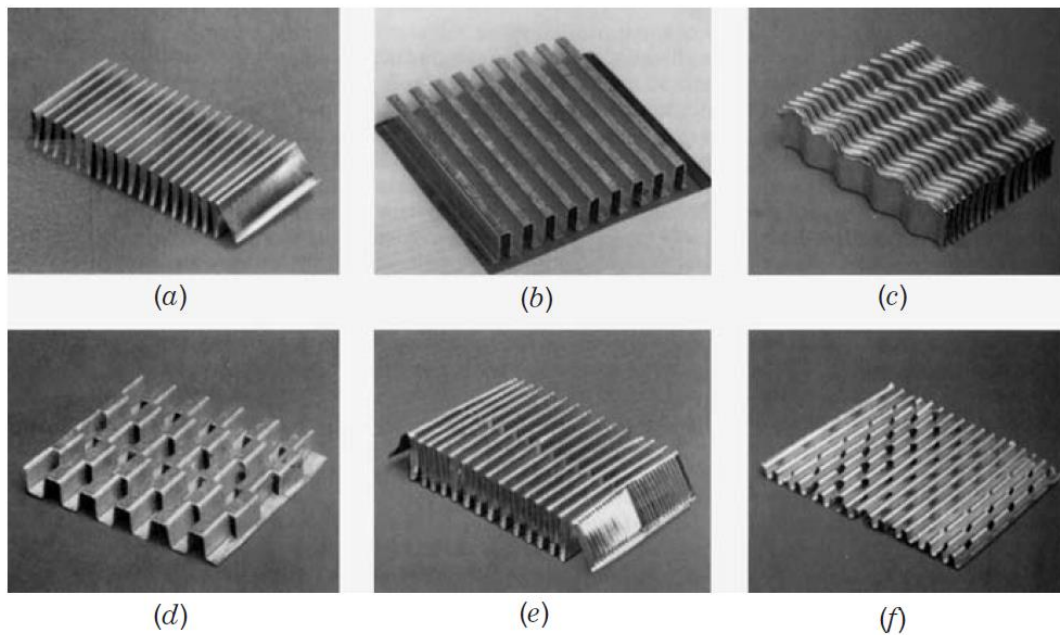


Figure 1.6 Various fin geometries for plate-fin heat exchangers: (a) plain triangular fin; (b) plain rectangular fin; (c) wavy fin; (d) offset strip fin; (e) multi-louvered fin; (f) perforated fin [7].

1.5 Aim of the Study

Intercoolers especially used in land vehicles are air-to-air crossflow compact heat exchangers. Because of having air on both flow sides, the suitable construction type for these intercoolers becomes plate-fin arrangement. With such a construction, the fin geometry of each flow side of the intercooler can be freely chosen depending on the requirements or limitations.

In this study, the main purpose is to theoretically examine the plate-fin geometries applicable to intercoolers. Each fin type shows different characteristic and thus leads to different intercooler performances. Evaluating these performance data enables comparison of fin geometries and determination of the most suitable ones for a given cooling duty.

A computer program is written for the theoretical calculations. All necessary parameters related with the fin geometries are embedded in this program. This speeds

up the laborious solution procedure of the performance data and provides extensive choice to the user in terms of fin variety.

Another purpose of this study is to illustrate the benefits of intercooling on engine performance; therefore the alteration of engine performance with the utilization of intercooler is established. Under some conditions intercooling becomes an impractical application and does not affect the engine operating parameters much. These conditions are demonstrated.

1.6 Review of Related Works

The performance characteristics of various fin geometries have been extensively investigated in terms of both first law and second law of thermodynamics. Heat transfer, pressure drop and second law performances (i.e. entropy generation, exergy destruction and second law efficiency) of them have been studied by researchers analytically, numerically and experimentally.

The most comprehensive experimental study has been established by Kays and London [8] with 132 compact heat exchanger surfaces. In the study, surfaces have been tested at certain Reynolds number ranges and their dimensionless heat transfer and friction factor parameters are determined. Results are given in graphical forms as a function of Reynolds number. Also, in this study the entrance and exit loss coefficients for different flow passage geometries are presented as a function of Reynolds number and contraction ratio.

In another study, London and Shah [9] have tested eight offset rectangular plate fin surfaces and presented basic heat transfer and flow friction characteristics of them. They also investigated nondimensional parameters characterizing the geometry of the fins and concluded that small offset spacing, small fin thickness and large aspect ratios are advantageous from heat transfer power versus flow friction power point of view. They also reported some important points related with application and fabrication of this type of surfaces.

Ismail et al. [10] have investigated flow patterns of compact plate-fin exchangers. The influence of flow maldistribution in the headers is examined numerically in the study. In order to improve the flow distribution, authors suggested to place punched baffles (plates) with different sized holes inside the header. They also generated dimensionless heat transfer and fluid friction data, for some offset and wavy fins, applicable for turbulent flow region.

Manglik and Bergles [11] have studied various offset strip fin surfaces and proposed new correlations for dimensionless heat transfer and fluid friction data that is both valid in laminar and turbulent region. They also compared these values with the existing experimental results in the literature and obtained agreement within $\pm 20\%$.

Another study related to offset strip fin correlations has been established by Kim et al. [12]. They have generated new sets of dimensionless heat transfer and fluid friction data that is also applicable to some fluids other than air. Also the geometries of offset strip fins in a fuel cooler were optimized with proposed correlations.

In another study, Li and Yang [13] have numerically investigated 3D models of offset strip fins and presented the effect of geometrical three-dimensionality on thermal-hydraulic performances. New correlations are proposed accounting the effect of third dimension and compared them with the existing experimental data. It is claimed that the proposed correlations are well adapted for offset strip fins with different fin thicknesses.

Cowell et al. [14] investigated performance characteristics of louvered fin surfaces and explained that; louvers do not generate turbulence and at high Reynolds numbers the flow has almost complete alignment with louvers. Also they compared louvered fins with offset strip fins and claimed that louvered fins are capable of outperforming offset strip fins.

Ryu and Lee [15] examined louvered fins both numerically and experimentally and suggested new correlations in terms of Reynolds number and ratio of fin pitch to louver pitch. They reported that these correlations are applicable to the surfaces having fin pitch to louver pitch ratios larger than 1.

Li and Wang [16] conducted an experimental study with new type of louver fins called multi-region louver fins and compared them with conventional ones. They suggested a new factor for comparison. It is claimed that some of the new louver fin types shows better performance than conventional ones. They also concluded that heat transfer coefficients and fluid friction factor tend to decrease with increased number of louver regions.

Vaisi et al. [17] have studied the effect of louver configuration on the heat transfer and pressure drop characteristics. They have carried out experiments by using symmetrical and asymmetrical arrangements of louver fins. It is reported that louvered fins with symmetrical arrangement provide 9.3% increment in heat transfer performance and 18.2% decrement in pressure drop. Also for a given heat transfer and pressure drop, the symmetrical arrangement ensures a 17.6% decrease in fin weight.

Ranganayakulu et al. [18] have investigated the effects of longitudinal heat conduction (LHC) on thermal performance in compact crossflow plate-fin, counterflow plate-fin, parallelflow plate-fin and crossflow tube-fin heat exchangers using a finite element method. They claimed that LHC is not always negligible in crossflow and counterflow compact heat exchangers especially when there is balanced flow and LHC parameter is larger than 0.005. Also it is reported that the performance deterioration in crossflow heat exchangers are higher than counterflow and parallelflow in all cases due to two dimensional wall temperature distribution in crossflow heat exchangers.

Ranganayakulu and Seetharamu [19] have conducted a finite element analysis on crossflow tube-fin heat exchangers and included the combined effects of LHC, inlet flow non-uniformity and temperature non-uniformity in their analysis. They have illustrated that, this combined effect is not always negligible especially when the capacity rates are equal and LHC parameter is larger than 0.05.

Shah and Skiepko [20] have conducted second law analysis on heat exchangers and illustrated the irreversibilities in terms of entropy generation. It is reported that effectiveness can be maximum, minimum or can have an intermediate value at the

maximum irreversibility point or effectiveness can be minimum or maximum at the minimum irreversibility point depending on the flow arrangement of two fluids. They have investigated the existence of entropy generation extrema and a relationship between extrema and the heat exchanger effectiveness for 18 different flow arrangements.

Gheorghian et al. [21] have proposed an entropy generation assessment criterion for compact heat exchangers and applied this criterion to totally 30 different heat transfer surfaces. They have investigated entropy generation rate caused exclusively due to change in heat transfer surface types and this made it possible to classify the surfaces in terms of entropy generation criterion. A comparison has been also made between proposed assessment criterion and augmentation entropy generation number criterion.

Canlı et al. [22] have compared three different compact heat exchangers in terms of second law of thermodynamics. They have experimentally evaluated heat transfer and pressure drop performance of the heat exchangers, and calculated the irreversibility and exergy efficiency of them using these data. The exergy efficiencies of the heat exchangers have been found between 15-40%. In the study, it is also concluded that increase in temperature difference results in larger entropy generation rate due to finite temperature difference, and by decreasing cooling fluid velocity, pressure drop and hence entropy generation rate due to fluid friction can be decreased.

CHAPTER 2

BASICS OF INTERCOOLERS

2.1 General Design Considerations of Intercoolers

The design of an intercooler mainly requires consideration of two parameters. These are heat transfer rate and pressure drop due to fluid friction. For effective cooling of intake air, intercoolers must be designed with a high surface area density. In fact this is a must for any gas-flow heat exchanger to compensate relatively low heat transfer coefficient of gases (low relative to most liquids). On the other hand, pressure drop of intake air due to fluid friction must be minimized. It adversely affects the charge air density and diminishes the benefits of supercharging.

To enhance heat transfer rate of an intercooler, surface area can be increased. However, this leads to larger size and higher cost. Another way of enhancing heat transfer rate is to increase the fluid flow velocity. In this case the increment rate will be something less than the first power of velocity but the increase in the fluid friction will be not less than the square of the velocity. This illustrates that there is a compromise between heat transfer rate and the fluid friction. Intercoolers should have a high frontal area and a short flow length to reduce pressure losses. A well-designed intercooler is the one that performs high heat transfer rate with a minimum pressure drop.

In intercoolers two different options are available in terms of cooling fluid type. Coolant can be liquid (water) or gas (air). Air-to-air cooling is preferred in most applications because it has some advantages over air-to-water cooling systems. Firstly, air is free and can be given back to atmosphere after passing through the intercooler whereas water must be cooled in a separate unit and requires a circulation pump for operation. Also fouling and corrosion can occur in water channels and this makes water treatment a necessity. Air-cooled systems mostly do not have fouling problems and corrosion is rarely seen [4].

Intercoolers are mounted on the engine and designed as an integral part of it. They should be as compact as possible not to hold much space in engine compartment. They are generally made of aluminum which is a lightweight material and has a good thermal conductivity. It has also good corrosion resistance [4]. The service life and maintenance periods of intercoolers must not be less than those of the basic engine [6].

2.2 Theory of Intercoolers

2.2.1 Thermal Design

In this section, beginning with the assumptions employed in the theory of heat exchanger design, the basic relations for the heat transfer analysis will be formulated.

2.2.1.1 Assumptions for Heat Transfer Analysis

Introducing a group of assumptions in heat transfer analysis provides to construct theoretical models that are easy enough to handle. For the analysis, the following assumptions and/or idealizations are proposed.

1. The heat exchanger operates under steady-state conditions, i.e. all the variables are independent of time.
2. Heat transfer only takes place between the fluids. The exchanger walls are insulated, i.e. no heat losses to or from the surroundings.
3. There is no generation or dissipation of thermal energy in the exchanger walls or fluids.
4. Wall thermal resistance is distributed uniformly in the entire exchanger.
5. Longitudinal heat conduction effects in the fluids and in the wall are negligible.
6. The individual or overall heat transfer coefficients are constant throughout the exchanger.
7. The velocity and temperature distribution over the flow cross-section is uniform.
8. Kinetic and potential energy of fluids are negligible.

2.2.1.2 Problem Formulation

In thermal analysis of heat exchangers two main approaches are possible. Theoretical models are built up using either the first law of thermodynamics (energy based analysis) or second law of thermodynamics (entropy/exergy based analysis). In energy based analysis, the effectiveness-number of transfer units (ε -NTU) or logarithmic mean temperature difference (LMTD) methods are commonly used to evaluate exchanger performance. On the other hand, in entropy/exergy based analysis various dimensionless parameters (see section 2.2.3) are derived to assess the quality of heat transfer and associated phenomena.

In this section thermal analysis of heat exchangers based on the first law of thermodynamics will be introduced. Later, the definition of effectiveness and ε -NTU relation for an air-to-air intercooler will be presented.

Consider a two-fluid counterflow heat exchanger shown in Figure 2.1. Two differential energy conservation equations for the control volume can be combined as follows:

$$dq = q'' dA = -C_h dT_h = -C_c dT_c \quad (2.1)$$

Here dq represents the differential amount of heat transfer rate from hot fluid to cold fluid through the differential wall surface area dA . The hot and cold fluids are denoted by subscripts h and c , respectively. The negative signs in the equation are a result of decreasing fluid temperatures in the direction of positive x . Heat capacity rate of the fluid is denoted by C and equal to the product of mass flow rate of fluid, \dot{m} and fluid specific heat at constant pressure, c_p .

$$C = \dot{m}c_p \quad (2.2)$$

The heat transfer rate equation (Eq. 2.1) can also be written in the form of:

$$dq = U(T_h - T_c)dA = U\Delta T dA \quad (2.3)$$

where U is the overall heat transfer coefficient. For this differential area, dA , the driving force for heat transfer is the local temperature difference $T_h - T_c = \Delta T$, and the overall thermal conductance is UdA .

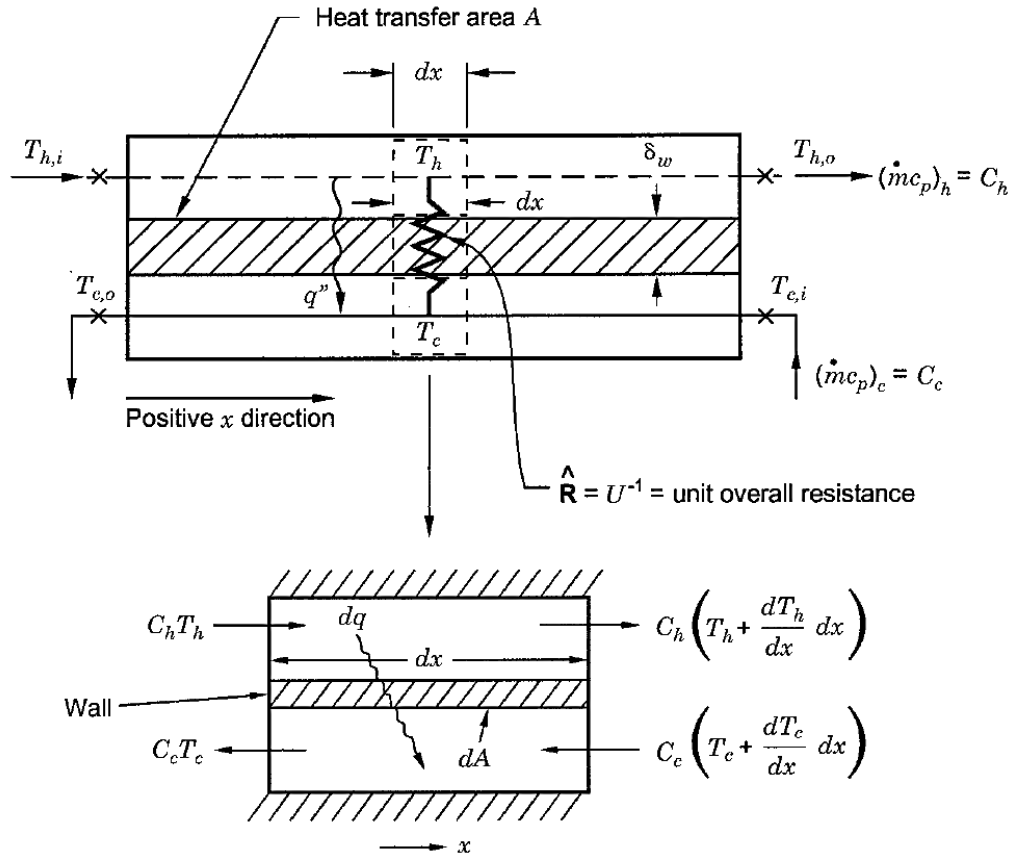


Figure 2.1 Depiction of heat transfer in a counterflow heat exchanger [7].

Integration of Eq. 2.1 and Eq. 2.3 over the entire heat exchanger surface for the specified inlet and outlet temperatures will give the expressions:

$$q = \int C dT = C_h(T_{h,i} - T_{h,o}) = C_c(T_{c,o} - T_{c,i}) \quad (2.4)$$

$$q = \int U \Delta T dA = UA \Delta T_m \quad (2.5)$$

The subscripts i and o in Eq. 2.4 represents the inlet and outlet, respectively. In Eq. 2.5, ΔT_m is the true (or effective) mean temperature difference between the fluids. U is considered as constant over the entire surface.

To evaluate overall thermal conductance, a thermal circuit is constructed. This yields to an expression in the form of:

$$\frac{1}{UA} = \frac{1}{(\eta_o hA)_h} + \frac{\delta_w}{k_w A_w} + \frac{1}{(\eta_o hA)_c} \quad (2.6)$$

In the equation, h is the convection heat transfer coefficient, k_w is the thermal conductivity of the wall, A_w is the wall conduction area and δ_w is the thickness of the wall. η_o represents the efficiency of extended (or total) surface and equal to unity when only primary surfaces (i.e. having no fins) are used. In this equation the fouling resistances are neglected on both sides of the flow.

ε -NTU Method

In an adiabatic heat exchanger, the thermal energy removed from the hot fluid is totally transferred to cold fluid. This provides a first law efficiency of 100% in such a system regardless of the amount of heat transferred. However, while designing a heat exchanger the main purpose is to transfer as much amount of heat as possible from hot fluid to cold one. Since the first law efficiency is insufficient to rate the heat transfer process in this manner, a new parameter called effectiveness is used. This parameter can take the maximum theoretical value of 1 and the larger the effectiveness, the greater amount of heat is transferred between the fluids.

In order to demonstrate effectiveness of a heat exchanger, firstly the maximum possible heat transfer should be evaluated. This limit could be achieved with a perfect counterflow heat exchanger that has an infinite surface area [4].

Consider that two fluid streams are flowing through a conventional direct-transfer type heat exchanger in opposite directions as in Figure 2.1. The maximum temperature difference in the exchanger is $\Delta T_{max} = T_{h,i} - T_{c,i}$. The heat transfer will reach to its maximum value when the cold fluid is heated to the inlet temperature of hot fluid or the hot fluid is cooled to the inlet temperature of cold fluid. Both cases cannot be reached simultaneously unless the heat capacity rates are equal. When $C_h \neq C_c$, which is usually the case, the fluid with the smaller heat capacity rate will

undergo a larger temperature change and hence it will be the first to experience the maximum temperature difference. At that instant heat transfer will stop. Therefore the maximum possible heat transfer becomes equal to:

$$q_{max} = C_{min}(T_{h,i} - T_{c,i}) \quad (2.7)$$

where C_{min} is the smaller of C_h and C_c [23]. It is deduced from the equation that the fluid having larger heat capacity rate will experience smaller temperature difference.

Effectiveness which is defined as the ratio of actual heat transfer rate to the maximum possible heat transfer rate can now be clarified.

$$\varepsilon = \frac{q_{act.}}{q_{max.}} = \frac{C_c(T_{c,o} - T_{c,i})}{C_{min}(T_{h,i} - T_{c,i})} = \frac{C_h(T_{h,i} - T_{h,o})}{C_{min}(T_{h,i} - T_{c,i})} \quad (2.8)$$

Effectiveness can also be expressed in terms of nondimensional groups.

$$\varepsilon = \phi \left(\frac{UA}{C_{min}}, \frac{C_{min}}{C_{max}}, flow\ arrangement \right) \quad (2.9)$$

Here the first dimensionless group is named as number of (heat) transfer units and second is heat capacity rate ratio.

$$NTU = \frac{UA}{C_{min}} \quad (2.10)$$

$$C^* = \frac{C_{min}}{C_{max}} \quad (2.11)$$

NTU designates the nondimensional heat transfer size or thermal size of the heat exchanger and thus it is a design parameter. Heat capacity rate ratio, C^* is an operating parameter since it is dependent on mass flow rate and temperatures of the fluids.

Effectiveness expressions in terms of NTU and C^* for different flow arrangements can be found in references [24, 25]. The expression that will be used in this study is given below. It is the one for unmixed-unmixed type crossflow heat exchangers.

$$\varepsilon = 1 - \exp\left\{\frac{NTU^{0.22}}{C^*} [\exp(-C^*NTU^{0.78}) - 1]\right\} \quad (2.12)$$

Note that for a given effectiveness and heat capacity rate ratio, the value of NTU in Eq. 2.12 cannot be determined without performing iterations.

2.2.2 Pressure Drop Analysis

In most applications fluids need to be pumped to move through the heat exchanger. It is therefore necessary to evaluate fluid pumping power expenditure as a part of the system design and operating cost analysis. Pumping power is proportional to the fluid pressure drop (or fluid friction) which in turn has a direct relationship with exchanger heat transfer, operation, size, mechanical characteristics and some other factors [7].

In the design of liquid-to-liquid heat exchangers, friction characteristics of the heat transfer surface is relatively unimportant because of the lower power requirement for pumping high density fluids. However, for gases, because of their low density, friction power greatly increases. It is important to have an accurate knowledge of friction characteristics of heat exchangers in gas-to-gas applications.

In intercoolers which are the subject of this study, the fluid pressure drop is an important design parameter and should be minimized. This minimization may be important in terms of operating cost but mainly it is essential to prevent decrement in air density. While evaluating the pressure drop in the intercoolers, the method available for the compact heat exchangers is adopted.

Total core pressure drop in compact heat exchangers can be examined in three main parts. These are core entrance pressure drop, core pressure drop and core exit pressure rise. To delineate better, a flow passage in a plate-fin heat exchanger is shown in Figure 2.2 along with the static pressure distribution. Here, the total core pressure drop between points 1 and 2 is given with the following expression.

$$\Delta P = \Delta P_{1-a} + \Delta P_{a-b} - \Delta P_{b-2} \quad (2.13)$$

The pressure drop between points 1 and a, ΔP_{1-a} is core entrance pressure drop and consists of two contributions: (1) The pressure drop due to flow area change, and (2) the pressure loss associated with free expansion that follows sudden contraction.

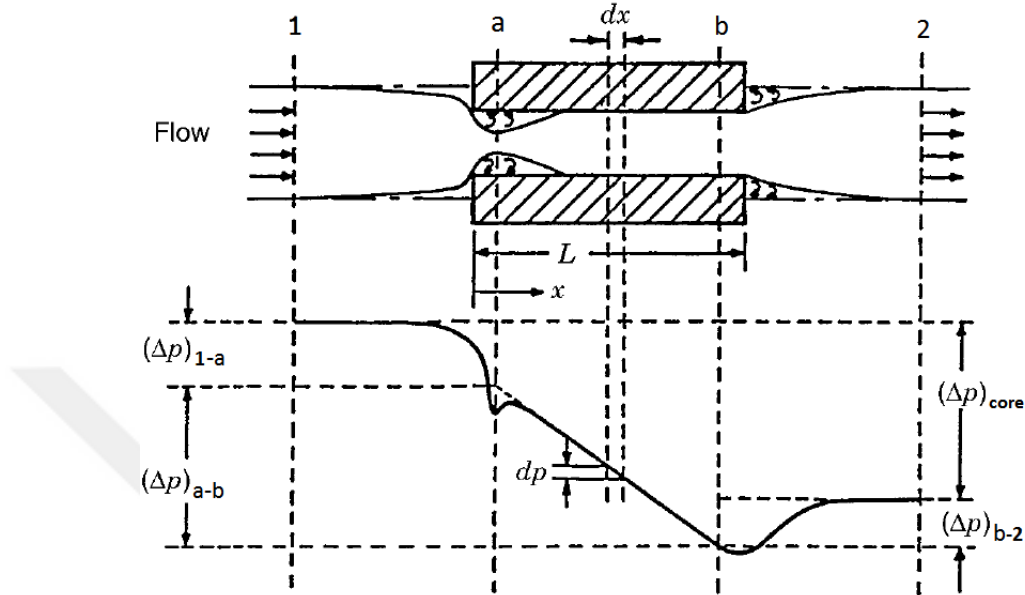


Figure 2.2 Pressure drop components in a plate-fin exchanger flow passage [7].

It may be mentioned at this stage that the change in pressure between point 1 and a is small compared to the total pressure, therefore density at point 1 and density at point a are taken equal to each other. The same case is also applicable between point 2 and point b. Hence:

$$\rho_1 = \rho_a \quad (2.14a)$$

$$\rho_2 = \rho_b \quad (2.14b)$$

Introducing σ as the ratio of free-flow area to frontal area, G as the core mass velocity and K_c as the entrance (contraction) pressure loss coefficient, ΔP_{1-a} is expressed in the form of:

$$\Delta P_{1-a} = \frac{G^2}{2\rho_1} (1 - \sigma^2 + K_c) \quad (2.15)$$

where:

$$G = \frac{\dot{m}}{A_o} = \rho_a V_a = \rho_b V_b \quad (2.16)$$

$$\sigma = \frac{A_o}{A_{fr}} \quad (2.17)$$

The core pressure drop, ΔP_{a-b} consists of two contributions that are (1) the pressure loss caused by fluid friction, and (2) the pressure change due to momentum rate change in the core. The expression for core pressure drop is:

$$\Delta P_{a-b} = \frac{G^2}{2\rho_1} \left[f \frac{A}{A_o} \rho_1 \left(\frac{1}{\rho} \right)_m + 2 \left(\frac{\rho_1}{\rho_2} - 1 \right) \right] \quad (2.18)$$

Here f is Fanning friction factor and A is heat transfer surface area. Also the fluid mean specific volume, v_m is determined using the relation:

$$\left(\frac{1}{\rho} \right)_m = v_m = \frac{v_a + v_b}{2} = \frac{1}{2} \left(\frac{1}{\rho_a} + \frac{1}{\rho_b} \right) \quad (2.19)$$

The core exit pressure rise, ΔP_{b-2} is also divided into two contributions: (1) pressure rise due to deceleration with an area increase, and (2) pressure loss associated with the irreversible free expansion and momentum rate changes following an abrupt expansion. It is similar to Eq. 2.15:

$$\Delta P_{b-2} = \frac{G^2}{2\rho_2} (1 - \sigma^2 - K_e) \quad (2.20)$$

In the equation, K_e is exit (expansion) pressure loss coefficient that is analogous to K_c . The values of both coefficients for different flow passage geometries are given in Figure D.1, in appendices.

Finally, by doing some manipulations, the total core pressure drop equation (Eq. 2.13) can be rearranged as:

$$\frac{\Delta P}{P_1} = \frac{G^2}{2\rho_1 P_1} \left[(1 - \sigma^2 + K_c) + f \frac{A}{A_o} \rho_1 \left(\frac{1}{\rho} \right)_m + 2 \left(\frac{\rho_1}{\rho_2} - 1 \right) - (1 - \sigma^2 - K_e) \frac{\rho_1}{\rho_2} \right] \quad (2.21)$$

Eq. 2.21 is used to evaluate the loss in the fluid pressure when flowing through the passage. It does not include the losses associated with fluid distribution devices such as inlet/outlet headers or manifolds.

Also note that satisfying the required heat transfer rate with a pressure loss limitation is referred as thermal-hydraulic design [25].

2.2.3 Second Law Analysis

As thermodynamics teaches us, all the processes that are not ideal are accompanied by entropy generation. It is an indicator of undesirable thermodynamic irreversibility that diminishes the available potential. This means that the presence of irreversibilities results in thermodynamic losses and leads to poorer thermal performance than the idealized reversible processes [7].

All the performance evaluation criteria presented up to now are based on the first law of thermodynamics, i.e. energy and mass balances. A different approach to quantify the heat exchanger performance is possible by identifying *thermodynamic quality* of the heat transfer and fluid flow processes in the exchanger [7]. Such an evaluation requires simultaneous use of both the first and second laws of thermodynamics. In order to assess a heat exchanger in this manner, formulation of irreversibilities in terms of entropy generation is necessary.

2.2.3.1 Irreversibilities in Heat Exchangers

The irreversibilities occurring in heat exchangers cause thermal performance deterioration. The more irreversibility involved, the poorer performance obtained. It disturbs the quality of the energy transfer. The amount of entropy generation expresses the degree of degradation due to irreversibility. Zero entropy generation,

which is the case for ideal processes, corresponds to the highest quality of energy transfer, and entropy generation greater than zero represents poorer quality [7].

There are two main important phenomena that shape the extent of generated entropy within a heat exchanger: (1) heat transfer through finite temperature difference and (2) fluid friction.

In order to evaluate total entropy generation rate in a heat exchanger, entropy balance equation is invoked. Considering heat exchanger as an adiabatic open system:

$$\dot{S}_{gen} = \Delta\dot{S} = \dot{m}_1\Delta s_1 + \dot{m}_2\Delta s_2 \quad (2.22)$$

Here the entropy change of a fluid stream can be expressed in a differential form using the canonical thermodynamic relation:

$$Tds = dh - v dP \quad (2.23)$$

where h is the specific enthalpy. For an ideal gas flow:

$$dh = c_p dT \quad (2.24)$$

$$Pv = RT \quad (2.25)$$

Substituting Eq. 2.24 and Eq. 2.25 into Eq.2.23 and integrating between inlet and outlet:

$$\Delta s = c_p \ln\left(\frac{T_o}{T_i}\right) - R \ln\left(\frac{P_o}{P_i}\right) \quad (2.26)$$

Eq. 2.26 is applied to both fluid streams and substituted into Eq. 2.22 to express the total entropy generation rate. Here, subscripts 1 and 2 denote fluid 1 and fluid 2, respectively. There is no need to specify which one is hot or cold fluid.

$$\begin{aligned} \dot{S}_{gen} = & (\dot{m}c_p)_1 \ln\left(\frac{T_{1,o}}{T_{1,i}}\right) - (\dot{m}R)_1 \ln\left(\frac{P_{1,o}}{P_{1,i}}\right) \\ & + (\dot{m}c_p)_2 \ln\left(\frac{T_{2,o}}{T_{2,i}}\right) - (\dot{m}R)_2 \ln\left(\frac{P_{2,o}}{P_{2,i}}\right) \end{aligned} \quad (2.27)$$

The significance of Eq. 2.27 will be much more obvious when it is broken into two parts. Grouping similar terms reveals that total entropy generation consists of two irreversibilities: (1) entropy generation due to heat transfer through finite temperature difference, and (2) entropy generation due to fluid friction. To illustrate this, Eq. 2.22 can be rewritten as:

$$\dot{S}_{gen} = \dot{S}_{gen,\Delta T} + \dot{S}_{gen,\Delta P} \quad (2.28)$$

where:

$$\dot{S}_{gen,\Delta T} = (\dot{m}c_p)_1 \ln\left(\frac{T_{1,o}}{T_{1,i}}\right) + (\dot{m}c_p)_2 \ln\left(\frac{T_{2,o}}{T_{2,i}}\right) \quad (2.29)$$

$$\dot{S}_{gen,\Delta P} = (\dot{m}R)_1 \ln\left(1 + \frac{\Delta P_1}{P_{1,o}}\right) + (\dot{m}R)_2 \ln\left(1 + \frac{\Delta P_2}{P_{2,o}}\right) \quad (2.30)$$

with a pressure drop term ΔP , defining the inlet and outlet pressure differences (i.e. pressure drop) of the each fluid side.

$$\Delta P = P_i - P_o \quad (2.31)$$

As mentioned before, the entropy generation means deterioration of thermal performance or in other words the loss of available potential. When available potential is mentioned, the concept of exergy comes into mind. Therefore it is also important to combine heat exchanger analysis with exergy concept. It is clear from thermodynamics that the entropy generation leads to exergy destruction and the relationship between them is given by Gouy-Stodola theorem [26].

$$\mathcal{D} = I = T_0 \dot{S}_{gen} \quad (2.32)$$

Here \mathcal{D} denotes the destroyed exergy (equivalent to irreversibility, I) and T_0 is the reference temperature.

2.2.3.2 Dimensionless Parameters

While evaluating the heat exchanger performance in terms of second law, two different evaluation techniques are offered: (1) evaluation technique using entropy as evaluation parameter, and (2) evaluation technique using exergy as evaluation parameter. Each technique has its own dimensionless parameters in different forms proposed by different investigators. In this section, some of these dimensionless parameters will be discussed.

In entropy based analysis, generally entropy generation rate is converted into dimensionless forms. One of the well-known dimensionless forms is called number of entropy generation units [27] or entropy generation number and defined as the ratio of the entropy generation rate to the maximum heat capacity rate.

$$N_s = \frac{\dot{S}_{gen}}{C_{max}} \quad (2.33)$$

When Eq. 2.33 is used for a balanced flow, the denominator (C_{max}) is replaced with heat capacity rate ($\dot{m}c_p$) of any stream [28]. The value of N_s can change between zero and infinity. As the value approaches the lower limit, one can conclude that the irreversibilities in the exchanger are getting lower.

Another dimensionless parameter also called entropy generation number is proposed by Hesselgreaves [29] and has the form of:

$$N_{s,1} = \frac{\dot{S}_{gen}}{q/T_1} \quad (2.34)$$

where T_1 is taken as the inlet temperature of cold stream.

Various augmentation techniques are applied to enhance heat transfer in heat exchangers. Augmentation entropy generation number [30] is the one that is used to evaluate performance of these techniques by comparing the entropy generation rates before and after augmentation. It is given by:

$$N_{s,a} = \frac{\dot{S}_{gen,a}}{\dot{S}_{gen,0}} \quad (2.35)$$

Augmentation techniques with $N_{s,a} < 1$ are thermodynamically advantageous since it both increases heat transfer and reduces the degree of irreversibility.

Similar to foregoing analysis, in exergy based evaluation technique, various nondimensional irreversibility parameters are used. A parameter called non-dimensional exergy destruction [31] is defined as:

$$I^* = \frac{I}{\dot{m}T_0c_p} \quad (2.36)$$

Another dimensionless measure of heat exchanger irreversibility can be calculated using the following equation:

$$\varepsilon_R = \frac{\dot{m}_c(\psi_{out} - \psi_{in})_c}{\dot{m}_h(\psi_{in} - \psi_{out})_h} \quad (2.37a)$$

Here ε_R is called rational (second law) effectiveness [32]. It has the maximum value of one when exergy gained by cold stream is equal to exergy donated by the hot stream, and this condition corresponds to the operation of the heat exchanger in a pure reversible manner. Note that when the temperature (or pressure) of the cold stream remains below the temperature (or pressure) of the surrounding during operation, it is better to use a more general definition instead of Eq. 2.37a. In such cases, Çengel [3] proposes to use:

$$\eta_s = \frac{(\dot{m}\psi_{out})_c + (\dot{m}\psi_{out})_h}{(\dot{m}\psi_{in})_c + (\dot{m}\psi_{in})_h} \quad (2.37b)$$

In this equation η_s is referred as second law efficiency. It is also known as rational efficiency or exergetic efficiency [33].

All these dimensionless parameters are commonly used in the literature by different investigators. More detailed review can be found in reference [33].

2.3 Some Additional Considerations for Thermal Design

2.3.1 Influence of Temperature-Dependent Fluid Properties

During the operation of heat exchangers, the temperatures of streams vary both over the flow cross section and in the flow direction. The change in the temperature affects the fluid properties (density, viscosity, specific heat etc.) and therefore the accuracy of thermal analysis. Some kind of correction is generally applied to recover the effect of temperature-dependent fluid properties.

The influence of temperature variation along the flow direction is compensated by evaluating the fluid properties at a mean temperature with respect to flow length. This is a typical case applied in the heat exchanger analysis. The arithmetic average of terminal temperatures is given by:

$$T_m = \frac{T_i + T_o}{2} \quad (2.38)$$

Eq. 2.38 is applied to hot and cold streams individually and fluid properties of each side are evaluated with respect to these mean temperatures.

To take into account the change in the temperature over the flow cross section, more elaborate correction scheme is presented. When the temperature difference between the fluid and heat transfer surface is large, fluid properties in the transverse direction to the flow vary considerably. This change in fluid properties may lead to significant variation in two important dimensionless parameters that are used in the assessment of heat exchanger performance: Nusselt number, Nu and friction factor, f [7].

To compensate it, the values of Nusselt number and friction factor evaluated at appropriate mean temperatures (Nu_m and f_m) are modified with the following expressions [8].

$$\frac{Nu}{Nu_m} = \left(\frac{T_w}{T_m} \right)^n \quad (2.39)$$

$$\frac{f}{f_m} = \left(\frac{T_w}{T_m}\right)^m \quad (2.40)$$

These expressions are valid for gas flows where T_w and T_m are absolute temperatures denoting the wall temperature (see Eq. 2.43) and mean fluid temperature, respectively. The exponents m and n have various magnitudes depending on the flow conditions and are summarized below in Table 2.1.

Table 2.1 Exponents of (T_w/T_m) [8].

	Heating	Cooling
<i>Laminar Flow</i>	$n = 0$ and $m = 1.0$	$n = 0$ and $m = 1.0$
<i>Turbulent Flow</i>	$n = -[\log_{10}(T_w/T_m)]^{1/4} + 0.3$ and $m = -0.1$	$n = 0$ and $m = -0.1$

The correction procedure used in liquid flows for temperature-dependent property effects is out of scope and not mentioned here.

2.3.2 Longitudinal Heat Conduction Effects

The exchanger theory presented up to this point is based on the idealization that there is no longitudinal heat conduction along the flow direction either in the fluids or in the separating wall.

In a heat exchanger, since heat transfer takes place, temperature gradients exist both in the fluids and in the wall. It means that heat conduction occurs in each fluid itself and in the wall along the flow direction. This may affect the heat transfer rate from hot fluid to cold fluid, i.e. effectiveness of the heat exchanger [7].

Heat conduction in the fluids is generally negligible due to their low thermal conductivity (except liquid metals), and therefore not covered in most applications. On the other hand, the heat conduction in the wall may be quite high and deteriorate the exchanger effectiveness substantially. The magnitude of heat conduction depends on the wall heat conductance and temperature gradient in the wall [7].

It can be proven that in a heat exchanger with longitudinal wall heat conduction, the effectiveness becomes function of following parameters.

$$\varepsilon = \phi[NTU, C^*, \lambda_h, \lambda_c, (\eta_o hA)^*, \text{flow arrangement}] \quad (2.41)$$

Here λ_h and λ_c are referred as the longitudinal wall heat conduction parameters for hot and cold fluid sides, respectively. They are defined in the form of:

$$\lambda_h = \left(\frac{k_w A_k}{LC} \right)_h \quad (2.42a)$$

$$\lambda_c = \left(\frac{k_w A_k}{LC} \right)_c \quad (2.42b)$$

Higher values of λ indicate greater rate of heat conduction in the wall.

The parameter $(\eta_o hA)^*$ denotes the ratio of cold side conductance to hot side conductance and used to evaluate wall temperature in the heat exchanger. Neglecting wall resistance and fouling, the wall temperature at any location can be written as:

$$T_w = \frac{T_h + (\eta_o hA)^* T_c}{1 + (\eta_o hA)^*} \quad (2.43)$$

where:

$$(\eta_o hA)^* = \frac{(\eta_o hA)_c}{(\eta_o hA)_h} \quad (2.44)$$

If $(\eta_o hA)^*$ is zero (as in a condenser) or infinity (as in an evaporator) the longitudinal heat conduction is zero even the value of λ is finite. Because in these cases, temperature of the wall becomes equal to phase-changing side temperature and it is constant. Longitudinal conduction effects are greatest when $(\eta_o hA)^*$ equal to unity [7].

Note that for a counterflow heat exchanger, the flow length and wall cross-sectional area of both sides are the same, therefore a unique longitudinal wall heat conduction parameter can be defined and Eq.2.41 can be simplified. Then, for a counterflow heat exchanger:

$$\lambda = \frac{k_w A_k}{LC_{min}} \quad (2.45)$$

$$\varepsilon = \phi[NTU, C^*, \lambda, (\eta_o hA)^*] \quad (2.46)$$

For unmixed-unmixed type crossflow heat exchangers, the temperature gradients in the wall in x and y directions of two fluid flows are different. Also hot side flow length is generally different than cold side flow length ($L_h \neq L_c$). In this case, effectiveness is a function of five independent parameters as given in Eq. 2.41 [7]. This makes the problem more complicated and yields evaluation in terms of numerical methods.

In the analysis of intercoolers as crossflow heat exchangers, tabulated numerical results given by Shah and Sekulic [7] can be used to take into account the effects of longitudinal wall heat conduction.

The effect of heat conduction in the wall is generally expressed in terms of reduction in the exchanger effectiveness ($\Delta\varepsilon/\varepsilon$) and defined as:

$$\frac{\Delta\varepsilon}{\varepsilon} = \frac{\varepsilon_{\lambda=0} - \varepsilon_{\lambda \neq 0}}{\varepsilon_{\lambda=0}} \quad (2.47)$$

2.3.3 Determination of Plate-fin Efficiency

In the analysis of intercoolers (or in any other extended surface heat exchangers), one of the important consideration is to evaluate the performance of fins that are used to increase surface area and hence the rate of heat transfer. Ideally, if fins are considered to have infinite thermal conductivity, the unfinned surface (also called primary surface or base surface) and finned surface temperatures will be equal. However, this is not the case in practice. Because of the finite value of thermal conductivity of the fins, the average temperature difference between fin and fluid is smaller when compared with the difference between base and fluid. This in turn leads to less heat transfer through fins than through primary surface. In order to take into account that effect, concept of fin efficiency, η_f and extended (or total) surface efficiency, η_o is introduced [7].

The efficiency of the fin is defined as the ratio of actual heat transfer to the maximum possible heat transfer through the fin. Such that:

$$\eta_f = \frac{q_f}{q_{f,max}} \quad (2.48)$$

Here the maximum possible heat transfer through fin, $q_{f,max}$. can be calculated considering base and fin temperatures as equal.

The total (finned and unfinned) surface performance is measured by the introduction of extended surface efficiency.

$$\eta_o = \frac{q_{total}}{q_{max.}} \quad (2.49)$$

where q_{total} includes both the heat transfer rate through the fin and the primary area. Maximum possible heat transfer rate again calculated presuming equal surface temperature for the fin and the base.

These two equations can be interrelated with the following form.

$$\eta_o = 1 - \frac{A_f}{A} (1 - \eta_f) \quad (2.50)$$

Here A_f is the fin surface area whereas A is the total surface area including fin and primary surface areas. Eq. 2.50 reveals that the determination of fin efficiency directly provides the value of surface efficiency.

Assessment of fin efficiency depends on the geometry of the fin and fin tip boundary condition [7]. Considering a thin, straight fin of uniform rectangular cross-section as in Figure 2.3 with adiabatic fin tip, the fin efficiency takes the form of:

$$\eta_f = \frac{\tanh ml}{ml} \quad (2.51)$$

where l is the length of the fin and:

$$m = \left(\frac{hP}{k_f A_{c,f}} \right)^{1/2} \quad (2.52)$$

Writing the relation for the perimeter, P and cross-sectional area, $A_{c,f}$ in terms of thickness of the fin, δ and fin flow length, L_f , Eq. 2.52 can be reorganized as given below.

$$m = \left[\frac{2h}{k_f \delta} \left(1 + \frac{\delta}{L_f} \right) \right]^{1/2} \approx \left(\frac{2h}{k_f \delta} \right)^{1/2} \quad (2.53)$$

The approximate term on the right hand side is valid when fin thickness is very small compared to fin flow length ($L_f \gg \delta$).

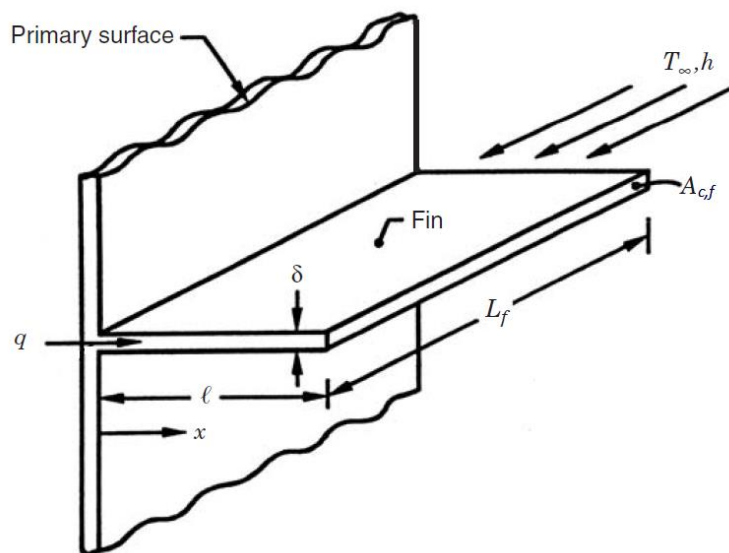


Figure 2.3 Straight, thin fin with uniform rectangular cross-section [7].

When plate-fin surfaces are considered the expressions given above are applicable with some modification. In most plate-fin heat exchangers, heat flow from (or to) both sides of a fin in the interior exchanger passages is idealized as symmetrical [7].

Consider two most commonly used plate-fin cross-sections, rectangular and triangular, as shown in Figure 2.4.

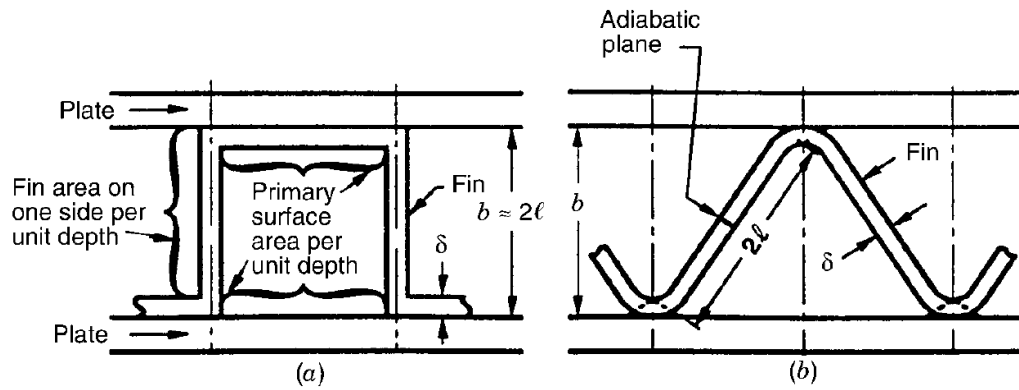


Figure 2.4 (a) Plain rectangular fin and (b) plain triangular fin [7].

For such passages, the fin efficiency is generally evaluated using Eq. 2.51. However, it is assumed that there is no heat transfer through the center of the fin (treated as adiabatic) and hence fin length is approximately taken equal to half of the plate spacing, b .

$$l = \frac{b - \delta}{2} \approx \frac{b}{2} \quad \text{or} \quad l = \frac{b - 2\delta}{2} \approx \frac{b}{2} \quad (2.54)$$

Here the approximate term in each formula is valid for b (or l) $\gg \delta$.

CHAPTER 3

DESIGN PROCEDURES OF INTERCOOLERS

From the quantitative analysis point of view, two important cases are encountered in thermal design of intercoolers (or any heat exchangers). These are rating and sizing problems [7]. In a rating problem the main purpose is to find the performance of an intercooler of given size under predetermined input conditions. This will tell us how effective the intercooler can operate (i.e. the extent of ability of it) under given conditions. This is why rating problem is also called performance problem. When the dimensions of an intercooler is not known but both input and required output conditions are known, this time the procedure yields a broad sense design and called sizing problem. The suitable dimensions (size) of the intercooler that satisfy the desired performance are determined at the end of the analysis. Both rating and sizing problems require an iterative solution procedure.

In this section, the stepwise solution procedures of these problems will be given. However, before explaining them, it is convenient to establish some specifications and operating conditions of the intercooler.

The construction type and flow arrangement is already known. Intercooler under discussion is unmixed-unmixed type crossflow heat exchanger having fins on both flow sides. On the other hand, there are numerous fin types (hence surface types) each having different geometry and performance characteristics in terms of heat transfer and fluid friction. Therefore the surface types for the intercooler must be elaborated first and then the operating conditions should be set up. The following two titles cover these topics. Later, rating and sizing procedures will be elucidated step by step.

3.1 Some Selected Surface Types and Their Characteristics

The plate-fin surfaces have various forms as mentioned in Chapter 1. The surfaces can be built with plain (triangular or rectangular), louvered, offset strip, wavy,

perforated and pin fins. Each of them has different geometry and exhibits different performance characteristics.

In this study, some (fin) surfaces investigated by Kays and London [8] will be used to construct the intercooler geometry. The effect of surface types on performance (in a rating problem) or dimensions (in a sizing problem) of the intercooler will be examined.

The selected surface types and their characteristics are given in Table A.1 in appendices. In order to denote each surface the notation given by reference [8] is used. Notations consist of numbers (sometimes numbers with letters) and have been created in such a way that, they give information about the dimensional characteristics of the fins in terms of inches. For example: Plain 12.00T denotes that this surface has fin density of 12 per inch and fins are triangular in shape. Some surfaces are designated with two separate numbers. The first refers to length of fin in flow direction; the second gives the fin density. This kind of notation is used in louvered and offset strip fins. For wavy fins, the first number is fin density and the second is the wavelength of the fin. Perforated fins are like plain fins and designated with a single number only.

3.1.1 Colburn Factor and Fanning Friction Factor

The basic data for heat transfer and pressure drop characteristics of compact heat exchanger surfaces are mostly obtained experimentally and hence introduced in terms of dimensionless parameters that are functions of Reynolds number. These parameters are Colburn factor (j factor) and Fanning friction factor (f factor), and denoted as:

$$j = St \cdot Pr^{2/3} = \phi_1(Re) \quad (3.1)$$

$$f = \frac{\rho \tau_w}{G^2/2} = \phi_2(Re) \quad (3.2)$$

Each surface type has different geometry, therefore exhibits a unique heat transfer and pressure drop performance. This reveals that each surface has its own value of j

and f factor and these values must be known to perform the analysis of the intercooler. For this reason, the experimental values of j and f factors tabulated by Kays and London [8] are gathered together for each selected surface. To minimize reading error and reduce the time of calculations, these tabulated data are curve-fitted as a function of Re and suitable equation models are extracted. For curve-fitting, least squares method is used and it is ensured that proposed equations gives coefficient of determination (R^2) value of at least 0.999 in all fittings. These equations are given in Table B.1 and Table B.2, in appendices. Reynolds number ranges at which the equations are valid are also given in Table B.3.

3.2 Operating Conditions of Intercooler

Identifying the operating conditions is an essential step before starting the intercooler analysis. In a rating problem in which the size of the intercooler is already known, determination of operating conditions requires knowing only the input conditions of each fluid side (hot and cold) in advance. Output conditions are evaluated at the end of the solution. However, in a sizing problem, both input and output conditions of each fluid side must be specified at the beginning of the analysis. The solution of the sizing problem gives the size of the intercooler.

It is already known that, the hot fluid is the charge air directed from the compressor of the turbocharger and the cold fluid is the ambient air. It is easy to specify the inlet properties of the ambient air which is considered to be at room temperature and one atmospheric pressure. Therefore cold side inlet temperature and pressure of the intercooler is 298.15 K and 101.325 kPa, respectively. Also the mass flow rate of cold fluid can be calculated considering the velocity of air (equal to vehicle speed) 90 km/h and cold side frontal area of the intercooler roughly 500x500 mm². This yields a mass flow rate of 3 kg/s for cold side. When it comes to hot side flow properties, more elaborated computation is required. The hot fluid passes through the compressor of the turbocharger and its pressure and temperature increases. Besides, the mass flow rate of it is arranged with respect to engine parameters. To go further some information related with the compressor and engine should be given. In this study, inlet conditions to the compressor are considered to be 298.15 K and 101.325

kPa and the pressure ratio (compression ratio of the compressor) is taken as 2.5. The air leaving the compressor is the hot side inlet of the intercooler. Figure 3.1 shows the air flow through the turbocharger, intercooler and the engine.

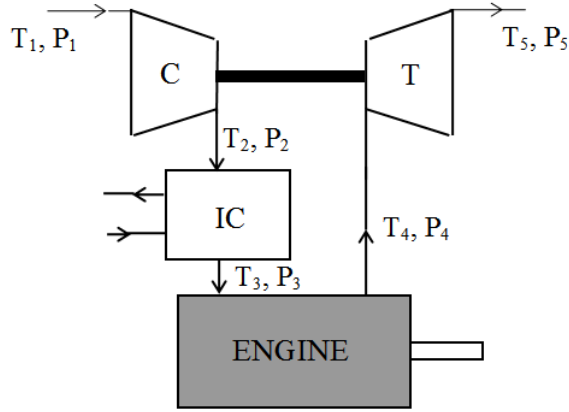


Figure 3.1 Charge air flow in a turbocharged and intercooled engine [4].

Assuming isentropic compression in the compressor, following expression can be written to find the exit temperature of air.

$$T_2 = T_1 \left(\frac{P_2}{P_1} \right)^{\frac{k-1}{k}} \quad (3.3)$$

Here k is the specific heat ratio and equal to 1.4. Using this relation the exit temperature of the air from the compressor is found to be 387.38 K where the exit pressure of it is easily calculated from pressure ratio information and equal to 253.313 kPa.

In order to evaluate the mass flow rate of charge air, engine specifications that belong to Ford Cargo TCI (TCI: turbocharged and intercooled) engine is used. Its technical details are given in Table 3.1. In addition to this, the hot fluid outlet conditions of the intercooler should be stated. It is supposed that there occurs 60 K of temperature drop and 1.5% pressure loss in the fluid during cooling. This yields 327.38 K exit temperature and 249.513 kPa exit pressure for the charge air leaving the intercooler.

Considering the engine is running at full speed (2780 rpm), eventually, mass flow rate of hot fluid can be calculated. The relation for mass flow rate:

$$\dot{m} = \frac{P}{RT} V_d \frac{N}{n} \quad (3.4)$$

Here V_d is total displacement volume of the engine, N is engine speed and n is the number of revolutions of the crankshaft for one thermodynamic cycle (equals to 2 for a four-stroke engine). Pressure and temperature values are decided previously and the value of R (specific gas constant of air) is 0.287 kJ/kg·K. Then, from Eq. 3.4 mass flow rate of charge air is found to be roundly 0.37 kg/s.

Table 3.1 Technical specifications of Ford Cargo TCI engine [Modified from 4].

Ford Cargo 6.0L TCI Diesel Engine	
Working cycle	4-Stroke
Number of cylinders	6
Cylinder bore (mm)	104.77
Cylinder stroke (mm)	114.9
Compression ratio	16.5
Engine brake power (kW)	136 (at 2400 rpm)
Maximum revolution (rpm)	2750-2780
Displacement volume (L)	5.947

With these evaluated parameters almost all inlet and outlet conditions of the intercooler is specified. There are two more important points to be mentioned. Firstly, it may not be important for the operation of the intercooler but, the pressure drop of cold fluid must be also specified to perform analysis in a sizing problem. It is assumed to have 1.5% pressure drop as in the case of hot fluid. Secondly, fixing the temperature drop of hot fluid fixes the value of effectiveness of the intercooler. The effectiveness becomes nearly 0.673 (67.3%), when the related parameters are substituted in Eq. 2.8. This value will be used as an input parameter in sizing problem.

3.3. Rating Problem

In a rating problem of an intercooler, the parameters to start the solution procedure are: surface type of each flow side, dimensions and input conditions of the hot and cold fluids. At the end of the solution, the output conditions and the effectiveness of the intercooler is obtained. The solution steps [7] are given below in details.

1. The surface geometry properties on each fluid side are determined using the characteristic information (see Table A.1) of the selected surface types and dimensions of the intercooler. Firstly, frontal area of both sides and total volume of the intercooler is determined with the following expressions.

$$A_{fr,h} = L_c L_{st} \quad (3.5a)$$

$$A_{fr,c} = L_h L_{st} \quad (3.5b)$$

$$V = L_h L_c L_{st} \quad (3.6)$$

Here L_h and L_c are hot and cold fluid flow lengths, respectively. L_{st} is the length called stack height (noflow height) as given in Fig. 1.5.

The ratio of heat transfer area of one side to total heat exchanger volume, α and ratio of free flow area to frontal area, σ of both sides can be calculated using the term after the second equality sign of the expressions:

$$\alpha_1 = \frac{A_1}{V} = \frac{b_1 \beta_1}{b_1 + b_2 + 2\delta_w} \quad (3.7)$$

$$\sigma_1 = \left(\frac{A_o}{A_{fr}} \right)_1 = \frac{b_1 \beta_1 (D_h/4)}{b_1 + b_2 + 2\delta_w} \quad (3.8)$$

Here b is plate spacing, β is surface area density, D_h is hydraulic diameter and δ_w is plate thickness. The values of first three terms are fixed when the surface type is chosen but the last term δ_w can be freely altered which is taken as 0.3 mm in this study.

Knowing the value of α and volume of the intercooler, the heat transfer surface area can be evaluated using Eq. 3.7. Same is valid for free flow area that can be found by putting the values of σ and frontal area into Eq. 3.8.

2. In this step, the fluid mean temperatures and thermophysical properties of each flow side is computed. Since the outlet temperatures are not known in a rating problem, initially an assumption for the exchanger effectiveness is necessary. It is generally taken between 50 and 75% for most single-pass crossflow exchangers [7].

Then outlet temperatures can be calculated such that:

$$T_{h,o} = T_{h,i} - \varepsilon \frac{C_{min}}{C_h} (T_{h,i} - T_{c,i}) \quad (3.9)$$

$$T_{c,o} = T_{c,i} + \varepsilon \frac{C_{min}}{C_c} (T_{h,i} - T_{c,i}) \quad (3.10)$$

While calculating heat capacity rate in foregoing equations, the specific heat values of fluids are taken equal to each other as a first approximation. Once the outlet temperatures are calculated in this way, specific heat values are updated with respect to mean temperatures and Eq. 3.9 and 3.10 is reevaluated. This procedure is repeated until the evaluated outlet temperatures have the same value with the ones that are used to calculate specific heat of fluids at mean temperature. After determining the true outlet temperatures, the thermophysical properties (c_p , μ , k and Pr) of both fluids are evaluated at the corresponding mean temperatures by using Table C.1 in appendices.

3. Next, the core mass velocity and Reynolds number of both fluid sides are evaluated by means of following equations.

$$G = \frac{\dot{m}}{A_o} \quad (3.11)$$

$$Re = \frac{GD_h}{\mu} \quad (3.12)$$

Reynolds number is used to determine the nondimensional heat transfer and flow friction characteristics (j and f factors) of selected surfaces. From equations given in Table B.1 and Table B.2, j and f factors of both sides are calculated. Then, to correct these two parameters for variable fluid property effects, Eq. 2.39 and Eq. 2.40 can be used. Conversion of j factor to Nu (Nusselt number) or vice-versa is done by the following expression.

$$j = \frac{Nu \cdot Pr^{-1/3}}{Re} \quad (3.13)$$

Note that in the first iteration of the solution since the wall temperature is not known and cannot be calculated without finding the heat transfer coefficient of both sides, it is not possible to correct j and f factors for variable fluid property effects. However, for the second and subsequent iterations the correction can be performed by using the values of the previous iteration.

4. From j and f factors, the heat transfer coefficients of both sides are computed by:

$$h = \frac{jGc_p}{Pr^{2/3}} \quad (3.14)$$

Later, the fin efficiency and extended surface efficiency of both sides are evaluated using Eq. 2.50, Eq. 2.51 and Eq. 2.53. At this point, material of the fins must be known to appoint their thermal conductivities. In this study, the aluminum fins having thermal conductivity of 238 W/m·K are used.

In order to find overall thermal conductance, the wall thermal resistance (R_w) must be evaluated using the following equation:

$$R_w = \frac{\delta_w}{k_w A_w} \quad (3.15)$$

The plate material is considered to be the same as fin material and hence k_w is known. However, to evaluate A_w , number of passages of both flow sides should be known.

Assuming N_p passages for the hot fluid and $(N_p + 1)$ passages for the cold fluid, stack height can be written as:

$$L_{st} = N_p b_h + (N_p + 1) b_c + (2N_p + 2) \delta_w \quad (3.16a)$$

In a rating problem L_{st} is known and hence the value of N_p can be found by writing Eq. 3.16a in the form of:

$$N_p = \frac{L_{st} - b_c - 2\delta_w}{b_h + b_c + 2\delta_w} \quad (3.16b)$$

Then the wall conduction area, A_w is calculated using the relation:

$$A_w = L_h L_c (2N_p + 2) \quad (3.17)$$

Finally, all necessary parameters are substituted into Eq. 2.6 to compute overall thermal conductance.

5. From the known heat capacity of each fluid side C^* is calculated using Eq. 2.11. Then the value of UA and C_{min} is substituted into Eq. 2.10 to find NTU . Lastly, the effectiveness of the heat exchanger is determined using Eq. 2.12.

6. In order to calculate the reduction in effectiveness due to the longitudinal wall heat conduction, two more parameters should be evaluated: λ and $(\eta_o hA)^*$.

To find λ_h and λ_c from Eq. 2.42a and Eq. 2.42b, respectively, the unknown term in these equations denoting the cross-sectional area for longitudinal heat conduction (A_k) must be evaluated. To compute A_k for hot and cold sides, following expressions are used, and then λ value of both sides is calculated.

$$A_{k,h} = 2N_p L_c \delta_w \quad (3.18a)$$

$$A_{k,c} = (2N_p + 2) L_h \delta_w \quad (3.18b)$$

The parameter $(\eta_o hA)^*$ is evaluated using Eq. 2.44. With the determined values of NTU , C^* , λ_h , λ_c and $(\eta_o hA)^*$, the reduction in effectiveness is found from the

tabulated data presented by Shah and Sekulic [7]. Finally the true effectiveness is computed from Eq. 2.47 and outlet temperatures are reevaluated using this value.

If new outlet temperatures are significantly different from those assumed at step 2, iteration is continued throughout the steps 2 to 6 until the assumed and computed outlet temperatures converge within the desired degree of accuracy.

7. With the ultimate value of the effectiveness obtained at the end of the iteration, the heat transfer rate can be calculated using the following expression.

$$q = \varepsilon C_{min}(T_{h,i} - T_{c,i}) \quad (3.19)$$

8. After evaluating all the correct values of previous steps, the pressure drop calculations are performed by using Eq. 2.21.

Firstly, fluid densities (reciprocal of specific volume) at the exchanger inlet and outlet are determined using ideal gas equation, Eq. 2.25. Since the outlet pressures are not known at this point, fluid outlet densities are calculated using the inlet pressures. The mean specific volume is the harmonic mean of inlet and outlet densities and evaluated from Eq. 2.19.

Then, f is corrected for variable fluid property effects by using Eq. 2.40 and K_c and K_e values are determined from Figure D.1.

Last, pressure drop of both sides are evaluated by using Eq. 2.21 and the outlet pressures are found. With these outlet pressures, the outlet densities are reevaluated and the pressure drop calculations are repeated until the outlet pressures used to find outlet densities converge within the certain degree of accuracy with the evaluated outlet pressures.

3.4 Sizing Problem

In a sizing problem of an intercooler, the surface type of each flow side, input conditions and also output conditions are known. The aim is to determine the

dimensions (i.e. size) of the intercooler satisfying the heat transfer and pressure drop requirements.

The solution steps [7] are given below in details.

1. In a sizing problem, generally desired effectiveness of the intercooler is specified instead of fluid outlet temperatures. In such a case, outlet temperatures is calculated by substituting specified effectiveness into the equations of step 2 of rating procedure and following the route in that step. After evaluating outlet temperatures, the fluid properties of both sides are determined.

2. Next, C^* and NTU is calculated from Eq. 2.11 and Eq. 2.12, respectively. Computing NTU requires iteration.

3. The first approximate value of the core mass velocity for each side is evaluated by means of given equation.

$$G = \left[\frac{2}{(1/\rho)_m \cdot Pr^{2/3}} \frac{\eta_o \Delta P j}{ntu f} \right]^{1/2} \quad (3.20)$$

Here η_o and j/f is assumed to be 0.8 and 0.3, respectively. ntu is taken equal to two NTU .

4. Using Eq. 3.12 Reynolds number of each flow side is evaluated, and from Table B.1 and Table B.2 j and f factors of selected surfaces are determined. The correction for variable fluid property effects is not applicable in the first iteration. For the following iterations it will be taken into account.

5. Heat transfer coefficients of both sides are computed from Eq. 3.14. The fin efficiency and extended surface efficiency of both sides are evaluated using Eq. 2.50, Eq. 2.51 and Eq. 2.53.

Then, overall heat transfer coefficient is calculated by the following expression:

$$\frac{1}{U_1} = \frac{1}{(\eta_o h)_1} + \frac{\alpha_1/\alpha_2}{(\eta_o h)_2} \quad (3.21)$$

Here α_1 and α_2 can be calculated from Eq. 3.7 and the ratio of them are equal to:

$$\frac{\alpha_1}{\alpha_2} = \frac{A_1}{A_2} \quad (3.22)$$

Note that in Eq. 3.21 the wall thermal resistance is ignored since the size of the heat exchanger is not known at this stage. For second and subsequent iterations it is computed from:

$$\frac{1}{U_1} = \frac{1}{(\eta_o h)_1} + \frac{\delta_w A_1}{k_w A_w} + \frac{A_1/A_2}{(\eta_o h)_2} \quad (3.23)$$

6. Now surface area, free flow area and core dimensions can be evaluated. In order to find the surface area:

$$A_1 = NTU \frac{C_{min}}{U_1} \quad (3.24)$$

Then, using Eq. 3.22, surface area of the other fluid side is easily calculated.

The longitudinal heat conduction effects are ignored in the first iteration since the exchanger size is not known yet. For subsequent iterations necessary parameters are calculated following the way as given in step 6 of rating problem and the reduction in effectiveness is found. In a sizing problem, the specified effectiveness is considered as the minimum effectiveness which the heat exchanger must provide. Therefore, NTU is updated to a larger value (by adding the reduction in effectiveness to the specified effectiveness and using Eq. 2.12) to compensate the deterioration of performance due to longitudinal heat conduction. The new value of NTU is then used in Eq. 3.24.

Next, the free flow area and the frontal area of each flow side are computed by the relations:

$$A_o = \frac{\dot{m}}{G} \quad (3.25)$$

$$A_{fr} = \frac{A_o}{\sigma} \quad (3.26)$$

Here σ can be found from Eq. 3.8. Finally to calculate flow length of hot and cold fluids:

$$L_1 = \left(\frac{D_h A}{4A_o} \right)_1 \quad (3.27)$$

Stack height (third dimension) is evaluated using either of two expressions:

$$L_{st} = \frac{A_{fr,1}}{L_2} \quad (3.28a)$$

$$L_{st} = \frac{A_{fr,2}}{L_1} \quad (3.28b)$$

7. Now, pressure drop of each flow side is to be calculated. It is done in a similar way as explained in step 8 of rating problem. Since pressure and temperature at inlet and outlet of each fluid is already known, fluid densities can be easily found from Eq. 2.25. The correction of f for variable fluid property effects and determination of K_c and K_e parameters are done as described in step 8 of rating problem.

Last, pressure drops of both fluids are evaluated and compared with the specified (or allowable) pressure drops. If the difference between these two is large, a new value of G for each fluid side is computed and the procedure is repeated from step 4 to step 7 until the evaluated pressure drops are equal to the specified ones. The new value of G for the next iteration is found using the following equation:

$$G_{new} = G \left(\frac{\Delta P_{specified}}{\Delta P} \right)^{1/2} \quad (3.29)$$

CHAPTER 4

RESULTS

This section is to be presented in three parts. In the first part, sizing procedure is performed on 20 different intercooler configurations. The characteristics of surface types given in Table A.1 and operating conditions explained in Chapter 3 have been utilized in this procedure. 15 number of intercooler configurations are built using same surface type (same fin geometry) on both flow sides and remaining 5 are set up such that, the surface type on one side is different than the surface type on the other side. Distinct configurations yield different dimensions as expected. Therefore, in this part it is possible to observe and compare these configurations in terms of dimensions when they have same operating conditions. Also the resulting configurations are examined to see whether or not they can satisfy the space requirements when installed into the engine compartment of a vehicle.

In the second part, a suitable reference size (hot flow length, cold flow length and stack height) for an intercooler is decided considering the size and weight limitations during installation. It is clear that a perfect intercooler with implausible dimensions is useless since its mounting on an engine compartment will not be possible. Therefore, in this part the reference size is set and all 20 configurations are considered to be at this size. The aim is to see their performance (in terms of first and second law of thermodynamics) when the same input conditions are applied to them. Later four of these configurations are chosen and the effect of mass flow rate on their performance is examined. Miscellaneous charts have been created for this purpose.

In the last part, intercooler is coupled to an engine and its effect on engine performance is explained. Here the purpose is to show the extent of improvements an intercooler (or a turbocharger intercooler combination) can provide to an engine. Also a discussion has been made to clarify whether or not intercoolers are always feasible to be utilized.

4.1 Sizing Results

The sizing results of 20 different intercooler configurations are given in Table 4.1.

In the table, the configurations 5, 11 and 16 are marked with asterisks to illustrate that Reynolds number ranges (see Table B.3 in appendices) for j and f factor equations are exceeded while sizing. Still, the solution is carried out and results are obtained. Note that this situation may seriously affect the accuracy of results depending on the amount of deviation from the limits.

The minimum volume is obtained when offset strip fin 1/9-24.12 is used on both flow sides. However, when its dimensions are examined it is clear that hot and cold side flow lengths are very short and hence difficult to achieve in practice. Also the stack height is very high (almost 3 meters) to become an automobile intercooler. In fact for this particular problem, it is the characteristic of all offset strip fins in which the flow lengths are very small but the stack heights are so excessive. This makes their usage unfeasible for this intercooling application. Moreover, it is worth to mention that the convection heat transfer coefficients of offset strip fins are superior to any other fin types as seen in Table 4.1.

When surfaces with louvered fins on both sides are considered, the volumes are larger than the ones with offset strip fins however; much more reasonable stack heights (especially in configurations 5 and 8) are achievable. The configuration 8 seems to have more plausible size and weight for an automobile intercooler application than other louvered fin configurations.

Using plain fins on both flow sides provide the smallest frontal areas among the first fifteen configurations. The volumes of these surfaces tend to have larger values than the ones that house louvered fins on both sides. Especially, having low fin density and large plate spacing, Plain 9.03 fin possesses less surface area density and therefore the first configuration has highest volume. Here the configurations 2 and 4 may satisfy the space requirements of an automobile intercooler better than other two.

Table 4.1 Sizing results of intercooler configurations.

Config. #	Fin type	L_h mm	L_c mm	L_{st} mm	V m^3	h_h $W/(m^2 \cdot K)$	h_c $W/(m^2 \cdot K)$
1	Plain 9.03 on both fluid sides	1021.5	122	129	0.01611	176.13	163.82
2	Plain 11.11 on both fluid sides	474.3	53.73	283.4	0.00722	233.89	210.39
3	Plain 19.86 on both fluid sides	277.1	30.85	527.14	0.00451	248.03	220.39
4	Plain 12.00T on both fluid sides	474.5	54	286.2	0.00733	214.86	193.6
5	Louvered 1/2-6.06 on both fluid sides*	374.8	47.46	420.86	0.00749	313.7	301.78
6	Louvered 3/8(a)-8.7 on both fluid sides	274	34.67	620	0.00589	334.57	321.5
7	Louvered 1/4-11.1 on both fluid sides	218.2	26.9	713.6	0.00419	399.45	380.17
8	Louvered 3/4-11.1 on both fluid sides	330.16	38.74	430.4	0.00551	306.32	281.07
9	Offset strip 1/8-15.61 on both fluid sides	156.53	19.35	980.6	0.00297	456.76	436.61
10	Offset strip 1/8-19.86 on both fluid sides	95.7	11.32	1730.2	0.00187	502.52	462.16
11	Offset strip 1/9-24.12 on both fluid sides*	66	7.9	2747.3	0.00143	533.13	499.26
12	Offset strip 1/10- 19.74 on both fluid sides	75.23	9.08	2413.2	0.00165	456.13	432.1
13	Wavy 11.5-3/8W on both fluid sides	189.5	23.5	897.7	0.00400	449.46	423.7
14	Wavy 17.8-3/8W on both fluid sides	165.42	20.53	972.4	0.00330	393.9	370.48
15	Perforated 13.95P on both fluid sides	227.2	24.26	711.1	0.00392	423.74	364.44

Table 4.1 (Continued) Sizing results of intercooler configurations.

Config. #	Fin type	L_h mm	L_c mm	L_{st} mm	V m^3	h_h $W/(m^2 \cdot K)$	h_c $W/(m^2 \cdot K)$
16	Plain 12.00T on hot fluid side, Plain 19.86 on cold fluid side*	405	37.53	378.1	0.00575	228.71	212.1
17	Plain 11.11 on hot fluid side, Louvered 3/4-11.1 on cold fluid side	429	42.62	340	0.00622	243	276.06
18	Plain 11.11 on hot fluid side, Offset strip 1/8-15.61 on cold fluid side	356.5	27.34	484.4	0.00472	260.53	400.72
19	Wavy 11.5-3/8W on hot fluid side, Plain 9.03 on cold fluid side	229.7	106.2	361.89	0.00883	416.84	183.11
20	Louvered 1/2-6.06 on hot fluid side, Louvered 3/4-11.1 on cold fluid side	340.7	44.04	432.14	0.00648	325.04	274.3

When wavy or perforated fins are used on both flow sides, the occupied volume by the intercooler is improved. They require less space than the ones having louvered or plain fins on both flow sides. Convection heat transfer coefficients of them are also striking. However, the stack height is too large to be useful or applicable.

Finally, when different fin geometries are preferred on two flow sides much more attractive results can be achieved in terms of intercooler dimensions. Of course, this requires proper selection of the type of fin geometry on each flow sides. As interpreted from Table 4.1, almost all the intercoolers that are set up with different fin types on two flow sides have the potential to be mounted readily to an engine compartment. Also the frontal areas of these configurations are comparable to ones that use plain fins on both sides. However, there occurs an exception for configuration 19 since it has the second largest volume (so significant weight penalty) and longest cold flow length (so largest hot side frontal area) of all configurations. This in fact proves that if fin geometry is not correctly chosen for the relevant flow side, the sizing results may be disappointing.

4.2 Rating Results

In order to compare the performance of 20 intercooler configurations given in Table 4.1, all of them must have the same input conditions and same dimensions. Input conditions are already determined as given in Chapter 3, therefore only a suitable reference size is left to be specified.

For rating problem, the dimensions of the intercooler is considered to be 500-50-400 mm denoting hot flow length, cold flow length and stack height, respectively. This size is determined considering the space and weight restrictions of the engine compartment.

4.2.1 Comparison in terms of Heat Transfer and Pressure Drop Performance

The results of thermal-hydraulic analysis are given in Table 4.2. Here the configurations 11 and 19 are marked with asterisks to illustrate that Reynolds number ranges (see Table B.3 in appendices) for j and f factors are exceeded while rating. Still, the solution is carried out and results are obtained. Note that this situation may seriously affect the accuracy of results depending on the amount of deviation from the limits.

The results of rating procedure illustrate that the effectiveness value is the highest, also closely approaches the maximum limit of 1, when offset strip fins are used on both sides of the flow. The main reason that makes offset strip fins efficient is the redeveloping laminar boundary layers due to interrupted fin surfaces that provide elevated heat transfer coefficients. They have 1.5 to 4 times higher heat transfer coefficients than those of plain fin geometries [7]. However, enhancing the heat transfer coefficients also gives rise to high friction factors and thus high pressure drops in offset strip fins. As seen from Table 4.2, the highest pressure drops are encountered in configurations having these fin types. The loss in pressure on hot fluid side approaches to 13% of its inlet pressure for configuration 11. Such an extreme loss cannot be tolerated in practice even if it displays the best heat transfer performance. Other configurations housing offset strip fins on both sides have hot side pressure losses ranging between 4-11% of their inlet pressures.

Table 4.2 Thermal-hydraulic performance results of intercooler configurations.

Config. #	Fin type	ε	q kW	ΔT_h K	ΔT_c K	ΔP_h Pa	ΔP_c Pa
1	Plain 9.03 on both fluid sides	0.433	14.45	38.63	4.78	1350.8	480.97
2	Plain 11.11 on both fluid sides	0.696	23.21	62.14	7.68	2395.5	681.54
3	Plain 19.86 on both fluid sides	0.854	28.45	76.21	9.42	4386.3	1073.7
4	Plain 12.00T on both fluid sides	0.693	23.11	61.85	7.65	2546.2	711
5	Louvered 1/2-6.06 on both fluid sides	0.742	24.72	66.2	8.18	4952	1038.7
6	Louvered 3/8(a)-8.7 on both fluid sides	0.83	27.65	74.05	9.15	7593	1456.4
7	Louvered 1/4-11.1 on both fluid sides	0.897	29.86	79.99	9.88	7626.7	1474.5
8	Louvered 3/4-11.1 on both fluid sides	0.809	26.94	72.15	8.92	3940.4	918.1
9	Offset strip 1/8-15.61 on both fluid sides	0.954	31.76	85.1	10.51	10318.8	1837.4
10	Offset strip 1/8-19.86 on both fluid sides	0.991	32.99	88.4	10.92	17630.3	3084.4
11	Offset strip 1/9-24.12 on both fluid sides*	0.998	33.23	89.03	11	31847.3	5124.9
12	Offset strip 1/10-19.74 on both fluid sides	0.996	33.16	88.85	10.98	28457.2	4630.7
13	Wavy 11.5-3/8W on both fluid sides	0.919	30.61	81.99	10.13	10240.2	1945.2
14	Wavy 17.8-3/8W on both fluid sides	0.945	31.49	84.36	10.42	10659.3	1970.5
15	Perforated 13.95P on both fluid sides	0.905	30.15	80.76	9.98	5814.3	1443.9

Table 4.2 (Continued) Thermal-hydraulic performance results of intercooler configurations.

Config. #	Fin type	ε	q kW	ΔT_h K	ΔT_c K	ΔP_h Pa	ΔP_c Pa
16	Plain 12.00T on hot fluid side, Plain 19.86 on cold fluid side	0.777	25.88	69.31	8.57	2505	1070.3
17	Plain 11.11 on hot fluid side, Louvered 3/4-11.1 on cold fluid side	0.756	25.19	67.44	8.34	2369	916.1
18	Plain 11.11 on hot fluid side, Offset strip 1/8-15.61 on cold fluid side	0.834	27.77	74.39	9.19	2334.2	1830.3
19	Wavy 11.5-3/8W on hot fluid side, Plain 9.03 on cold fluid side*	0.593	19.79	52.95	6.55	25229.7	199.44
20	Louvered 1/2-6.06 on hot fluid side, Louvered 3/4-11.1 on cold fluid side	0.778	25.92	69.41	8.58	4923	916.9

Another interrupted fin type, louvered fins provide good heat transfer and pressure drop characteristics when used on both sides of the flow. The effectiveness of them ranges between 0.74-0.90. The highest pressure drop on hot flow side is around 3% which is much more less than most of the offset strip fins. If combination of high heat transfer rate and low pressure drop is mandated, choosing configuration 8 seems to be more reasonable than the other ones. It can maintain nearly 1.5% pressure drop on hot fluid side with a substantial effectiveness value of 0.809. Configurations 6 and 7 have higher effectiveness values but pressure losses are also higher.

Configurations with wavy and perforated fins show even better heat transfer rates than the ones having louvered fins on both sides. However, the pressure loss of fluids inside the core is again large, especially for the intercoolers housing wavy fins.

Plain fins exhibit different performance features when used on both sides of the flow. Configuration 1 has the lowest effectiveness among all configurations whereas configuration 3 has comparable heat transfer performance. This condition is in fact due to discrete characteristics of their fin geometries. Plain 9.03 has large plate spacing and low fin density therefore provides less surface area density. This results

in low heat transfer rate in this configuration. On the other hand, having smaller mass velocity and larger hydraulic diameter, the pressure drop becomes very small (less than 1% on both sides). The opposite is true for Plain 19.86 therefore configuration 3 offers high effectiveness but also high pressure drop. The remaining two configurations have average heat transfer performances together with quite acceptable pressure drops.

Finally, configurations having different fin geometries on two fluid sides can be considered to have adequate performance in terms heat transfer and pressure drop with an exception of configuration 19. It has somehow very high pressure drop on hot fluid side (almost 10%) and keeps itself out of the acceptable limits. Configuration 18 in fact seems to be the one of the best available intercooler with its remarkable performance.

If the output conditions of the configurations in Table 4.2 are also assessed to see whether or not they fulfill the desired output conditions of sizing procedure (60 K or higher temperature drop on hot fluid side and 1.5% or less pressure drop on both flow sides), only a limited number of them can satisfy the requirements. These are configuration 2, 4, 16 and 17.

4.2.2 Comparison in terms of Second Law of Thermodynamics

In this part using the heat transfer and pressure drop data given in Table 4.2, the performance of the configurations in terms of second law of thermodynamics is presented. Total entropy generation rate \dot{S}_{gen} and second law efficiency η_s of them are calculated for this purpose using Eq. 2.27 and Eq. 2.37b, respectively.

As mentioned earlier entropy generation due to finite temperature difference and entropy generation due to fluid friction form the total entropy generation in heat exchangers. Therefore in order to see the extent of these contributions to the total entropy generation rate, $\dot{S}_{gen,\Delta T}$ and $\dot{S}_{gen,\Delta P}$ are also computed. The results are given in Table 4.3.

Table 4.3 Second law performance results of intercooler configurations.

Config. #	Fin type	ϵ	η_s	\dot{S}_{gen} kW/K	$\dot{S}_{gen,\Delta T}$ kW/K	$\dot{S}_{gen,\Delta P}$ kW/K
1	Plain 9.03 on both fluid sides	0.433	0.8792	0.01345	0.00878	0.00466
2	Plain 11.11 on both fluid sides	0.696	0.8349	0.01838	0.01156	0.00682
3	Plain 19.86 on both fluid sides	0.854	0.7916	0.02319	0.01217	0.01103
4	Plain 12.00T on both fluid sides	0.693	0.8322	0.01867	0.01154	0.00714
5	Louvered 1/2-6.06 on both fluid sides	0.742	0.7953	0.02279	0.01182	0.01097
6	Louvered 3/8(a)-8.7 on both fluid sides	0.83	0.75	0.02783	0.01213	0.01570
7	Louvered 1/4-11.1 on both fluid sides	0.897	0.7479	0.02806	0.01219	0.01587
8	Louvered 3/4-11.1 on both fluid sides	0.809	0.8061	0.02158	0.01208	0.00950
9	Offset strip 1/8-15.61 on both fluid sides	0.954	0.7099	0.03229	0.01212	0.02017
10	Offset strip 1/8-19.86 on both fluid sides	0.991	0.5841	0.04628	0.01200	0.03428
11	Offset strip 1/9-24.12 on both fluid sides*	0.998	0.3626	0.07093	0.01198	0.05896
12	Offset strip 1/10-19.74 on both fluid sides	0.996	0.4167	0.06492	0.01199	0.05293
13	Wavy 11.5-3/8W on both fluid sides	0.919	0.7013	0.03325	0.01217	0.02107
14	Wavy 17.8-3/8W on both fluid sides	0.945	0.698	0.03361	0.01213	0.02147
15	Perforated 13.95P on both fluid sides	0.905	0.7573	0.02700	0.01218	0.01482

Table 4.3 (Continued) Second law performance results of intercooler configurations.

Config. #	Fin type	ϵ	η_s	\dot{S}_{gen} kW/K	$\dot{S}_{gen,\Delta T}$ kW/K	$\dot{S}_{gen,\Delta P}$ kW/K
16	Plain 12.00T on hot fluid side, Plain 19.86 on cold fluid side	0.777	0.8001	0.02217	0.01197	0.01020
17	Plain 11.11 on hot fluid side, Louvered 3/4-11.1 on cold fluid side	0.756	0.814	0.02070	0.01188	0.00882
18	Plain 11.11 on hot fluid side, Offset strip 1/8-15.61 on cold fluid side	0.834	0.7411	0.02881	0.01213	0.01668
19	Wavy 11.5-3/8W on hot fluid side, Plain 9.03 on cold fluid side*	0.593	0.7883	0.02356	0.01072	0.01284
20	Louvered 1/2-6.06 on hot fluid side, Louvered 3/4-11.1 on cold fluid side	0.778	0.8034	0.02189	0.01198	0.00991

Since the accuracy of the results in this part is dependent on the accuracy of the heat transfer and pressure drop values given in Table 4.2, the configurations 11 and 19 are also marked with asterisks in Table 4.3.

The evaluation in terms of second law reveals some interesting outcomes when the table is carefully examined. First of all, it is clear that the configuration 11 which has highest effectiveness value among all configurations in fact gets the worst ranking when assessed in terms of second law efficiency. \dot{S}_{gen} value of this configuration is the largest which holds it in the worst place since entropy production is directly proportional to exergy destruction. The leading contribution to entropy generation comes from the excessive pressure loss of fluids or in other words the generated entropy due to fluid friction. This situation is actually characteristics of the configurations having offset strip fins on both flow sides. Therefore most of them have lower second law efficiency values when compared to other configurations.

Having lower pressure drop values the configurations with louvered fins on both flow sides display better second law performances than the ones with offset strip fins. The contributions of $\dot{S}_{gen,\Delta T}$ and $\dot{S}_{gen,\Delta P}$ to total entropy generation rate are

pretty much same in these configurations. Also, an interesting situation arises in configuration 7. It has the largest finite temperature difference entropy generation among all configurations although the largest temperature changes in hot and cold fluids are not reached in this configuration.

Wavy and perforated fins leads to high pressure drops, therefore $\dot{S}_{gen,\Delta P}$ provides larger contribution to the total entropy generation in configurations having these fins on both flow sides. The configuration housing perforated fins have lower entropy generation and hence higher η_s value than other two.

Intercoolers with different fin types on hot and cold flow sides exhibit similar second law characteristics. Here remarkable point to mention is that, configuration 19 has very large pressure drop on hot fluid side (see Table 4.2) but due to low mass flow rate of hot fluid, it has less entropy generation rate than configuration 18.

When configurations having plain fins on both flow sides are investigated, attention should be given to configuration 1. It exhibits the best performance when assessed in terms of second law efficiency and provides the lowest entropy generation rate within 20 configurations. However, in terms of thermal performance it has the lowest effectiveness value and therefore poorest heat transfer. By looking at these results someone could have a misleading perception such that; using a configuration with low effectiveness maintains high second law efficiency and vice versa. This statement is of course incorrect and true outcome is reached with the detailed examination of the second law efficiency expression. In order to attain the maximum value of η_s from Eq. 2.37b there are two ways. First, if there is no heat transfer and pressure drop in the heat exchanger the second law efficiency becomes maximum, 1. The sum of output exergies will be equal to sum of input exergies since there is no change in the fluid exergies. This situation in fact creates a contradiction to the heat exchanger's raison d'être. The other way is the reasonable one; transferring exergy of hot fluid to cold fluid in a reversible manner and hence accomplishing the process with the maximum possible second law efficiency. It is actually what a heat exchanger must try to do.

Consequently, two important conclusions can be attained with these explanations. First, since fluids passing through configuration 1 experience the least amount of heat transfer and pressure drop (therefore produces small amount of irreversibility), the second law efficiency of this process appears to be very high. But in fact it operates with a low effectiveness and hence shows poor performance in terms of heat transfer. Second, in order to avoid such contradictory results while analyzing the second law characteristics of heat exchangers in terms of second law efficiency, it could be better to use Eq. 2.37a instead of Eq. 2.37b.

As final words of this part; it is clear that if there is no entropy generation and hence exergy destruction (ideally achievable with infinite surface area and zero pressure drop), a heat exchanger will be performing its duty perfectly. However, the entropy generation cannot be eliminated in these configurations even if they have infinite heat transfer area and zero core pressure drop. It is due to the fact that, the configurations do not have equal heat capacity rates and thus, at the end of the heat exchange process, the cold fluid outlet temperature cannot be equal to hot fluid inlet temperature. This will create an inevitable irreversibility called remanent or flow imbalance irreversibility. In other words, the high quality fluid (hot fluid) will be transformed to a low quality one during heat transfer and the cold fluid cannot be raised to the same high quality at the exit of the intercooler because of its higher heat capacity rate. Therefore the exergy destruction becomes unavoidable during the process. To sum up, the second law efficiency of these configurations could attain its maximum theoretical value only if the intercooler is ideal and hot and cold fluids have equal heat capacity rates (i.e. balanced flow).

4.2.3 Variation of Performance Parameters with Mass Flow Rate

Four configurations, namely configuration 1, 8, 9 and 16 having reference size are to be examined in this part. All the input parameters explained before are held constant except mass flow rate of hot fluid which is altered from 0.1 to 0.5 kg/m³. The purpose is to investigate the influence of mass flow rate on their effectiveness, hot side pressure drop, hot side outlet density and second law characteristics by means of charts.

Firstly, in Figure 4.1 variation of effectiveness with respect to mass flow rate is presented. Here effectiveness values of all configurations are decreasing as the hot side mass flow rate is increased.

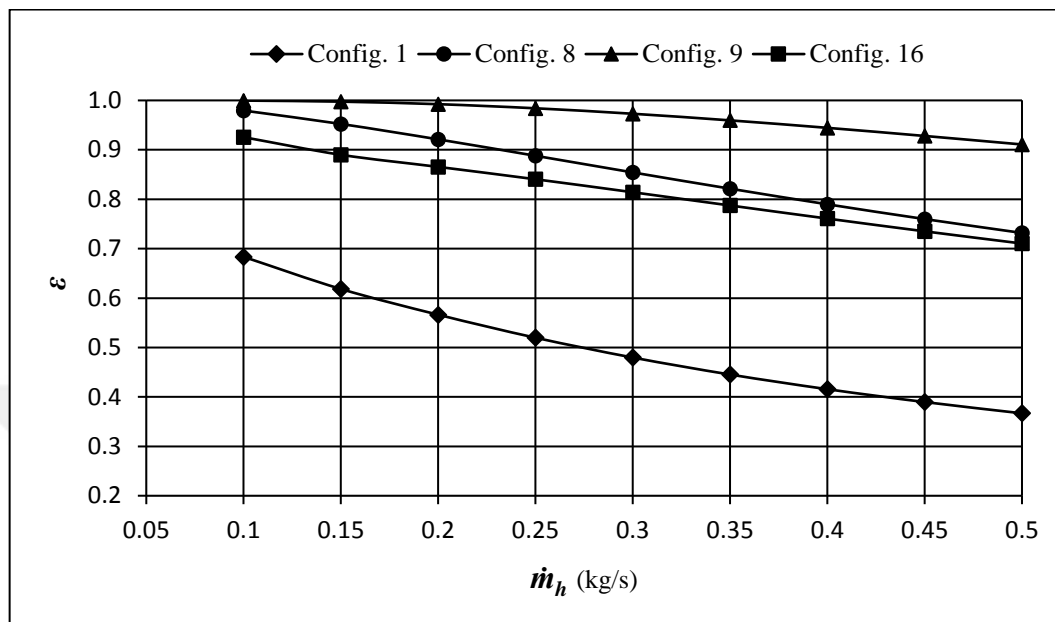


Figure 4.1 The change of effectiveness with respect to hot side mass flow rate.

Such a behavior can be explained with the following statements. As the mass flow rate increases in the core, the velocity and hence the overall heat transfer coefficient increases. This provides larger amount of heat transfer. However, the increment rate in overall heat transfer coefficient (or overall thermal conductance) is always less than the one in hot side mass flow rate (or minimum heat capacity rate) and hence there occurs a reduction in NTU . Lower NTU value leads to lower effectiveness.

Additionally, when configurations are compared the highest thermal performance rank is kept by configuration 9 which has offset strip fins on both flow sides. Also the decrement rate of effectiveness in this configuration is much more less than the others. This is due to fact that; the change in effectiveness with respect to NTU is small at high values of NTU .

In Figure 4.2, hot side pressure drops are compared. It is obvious that, increasing mass flow rate advances G on hot side since the free flow area is constant. Pressure drop is directly proportional to G^2 and hence it also increases. This situation explains the rise in the pressure drop when the mass flow rate gets larger. Moreover, because of having higher friction factor than the rest of the configurations, configuration 9 has the largest pressure loss.

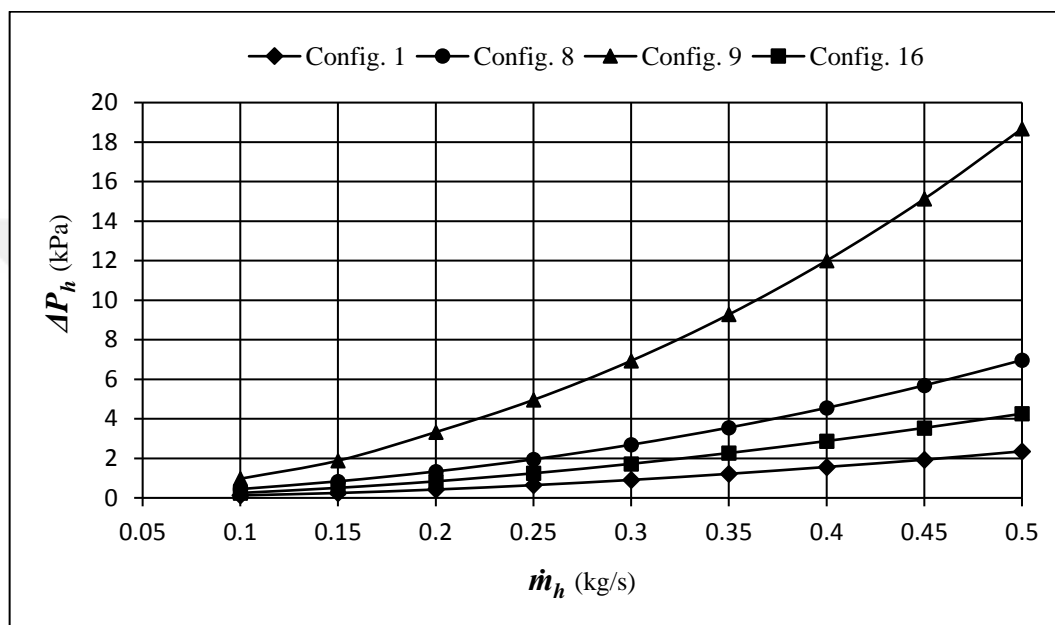


Figure 4.2 The change of hot side pressure drop with respect to hot side mass flow rate.

When the hot side outlet density is examined, it shows a downward trend with mass flow rate in all given configurations as seen in Figure 4.3. The lowest density is obtained in configuration 1. It has least effectiveness therefore hot fluid outlet temperature becomes highest and outlet density becomes lowest. In configuration 9, a sharp decrease occurs with increase in mass flow rate. This is in fact the result of high pressure drop in the hot fluid. Configuration 9 results in much lower outlet pressures as the mass flow rate of hot fluid increases. This decreases the density quite a lot.

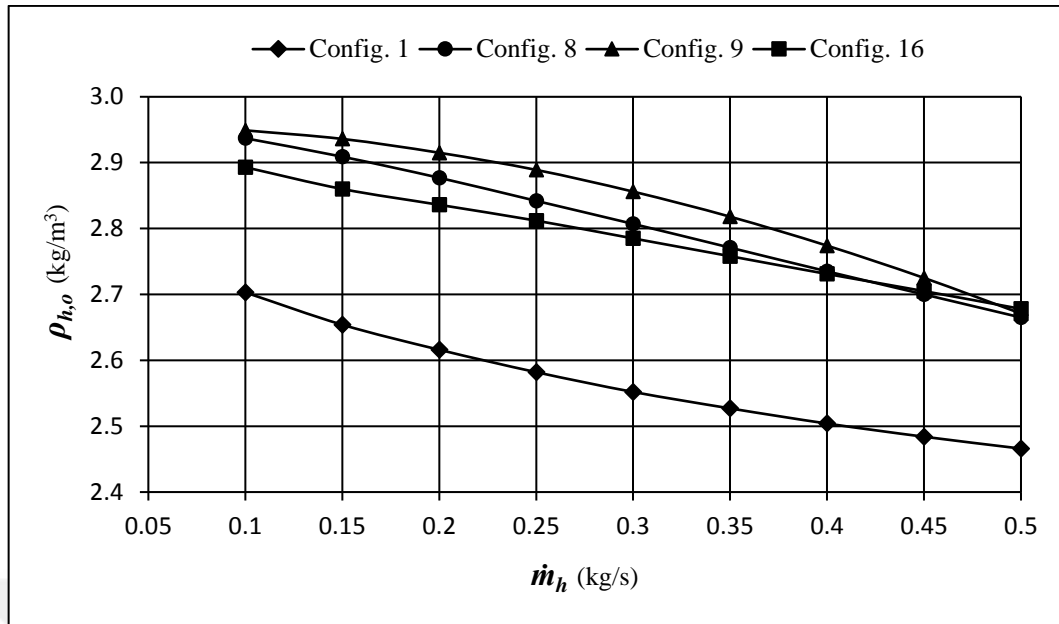


Figure 4.3 The change of hot side outlet density with respect to hot side mass flow rate.

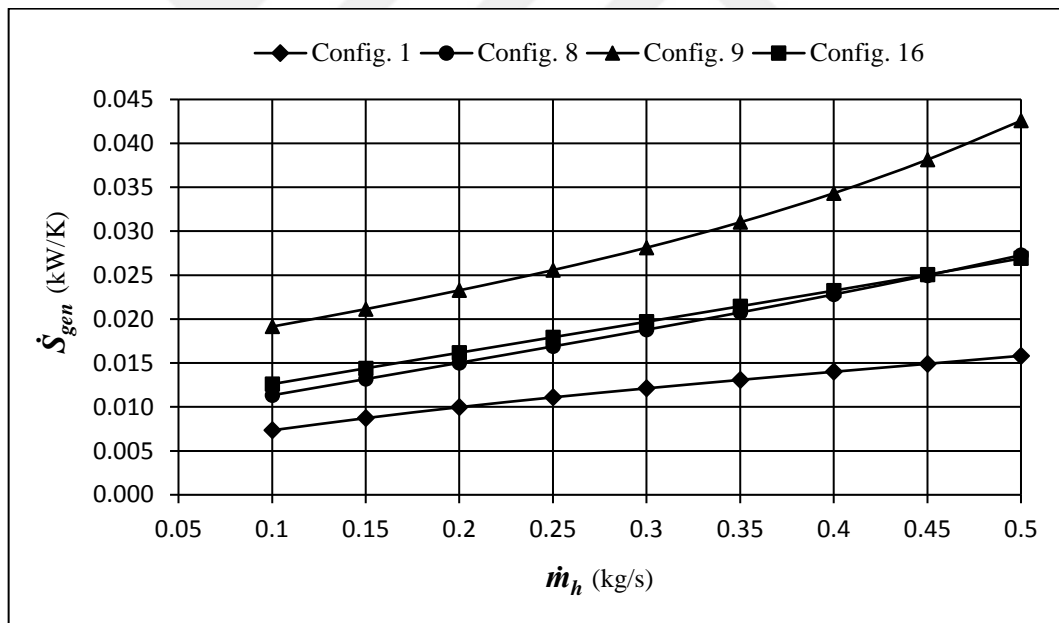


Figure 4.4 The change of total entropy generation rate with respect to hot side mass flow rate.

Delivering larger flow rate to the intercoolers increases total entropy generation rate as shown in Figure 4.4. It is an expected outcome since mass flow rate and total entropy generation rate is directly proportional. The highest entropy production rate

is observed in configuration 9. In this configuration, offset strip fins lead to high pressure losses (see Fig. 4.2) and hence largest contribution to total entropy generation rate is provided by the fluid friction. Configurations 8 and 16 have close \dot{S}_{gen} values as seen in the figure, but the increment rate of configuration 8 is slightly higher.

In Figure 4.5 the change of normalized (or nondimensional) entropy generation rate with respect to mass flow rate is given. To obtain the normalized form, entropy generation rate is divided by minimum heat capacity rate (hot side heat capacity rate). Neglecting slight variation in the specific heat of hot fluid, actually this graph illustrates that the entropy generation per unit mass flow rate decreases as \dot{m}_h increases.

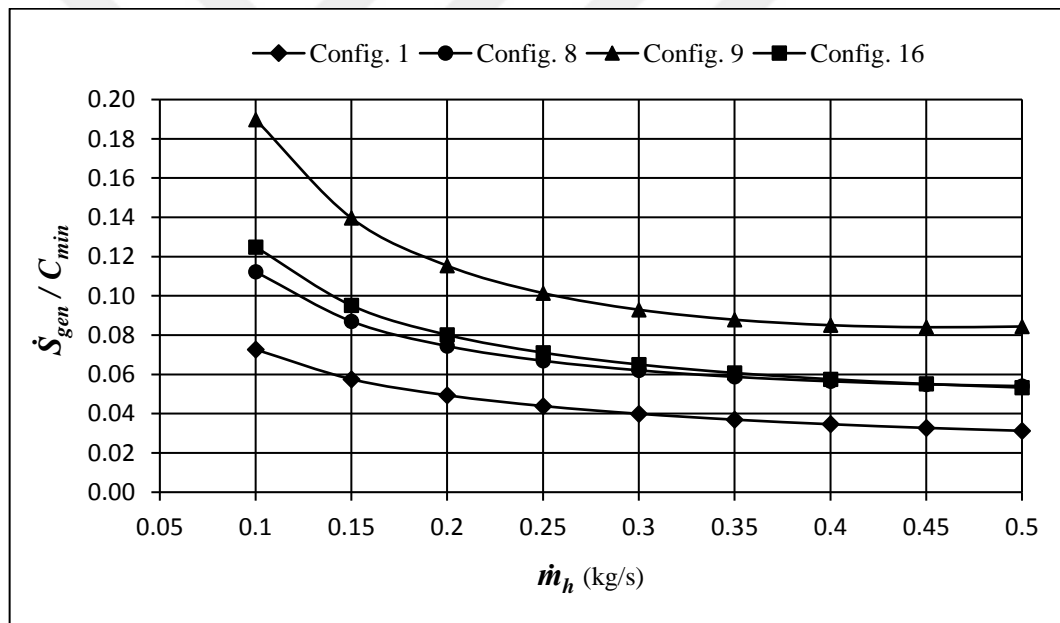


Figure 4.5 The change of normalized entropy generation rate with respect to hot side mass flow rate.

Presenting the second law efficiency characteristics of configurations in Figure 4.6, the previous two charts draw more attention. It is plausible to interpret all of them together. Someone looking at Figure 4.4 can reach a conclusion that the second law efficiency decreases as the mass flow rate increases, however this is not the case as

seen in Figure 4.6. The second law efficiency has an increasing trend as the mass flow rate increases.

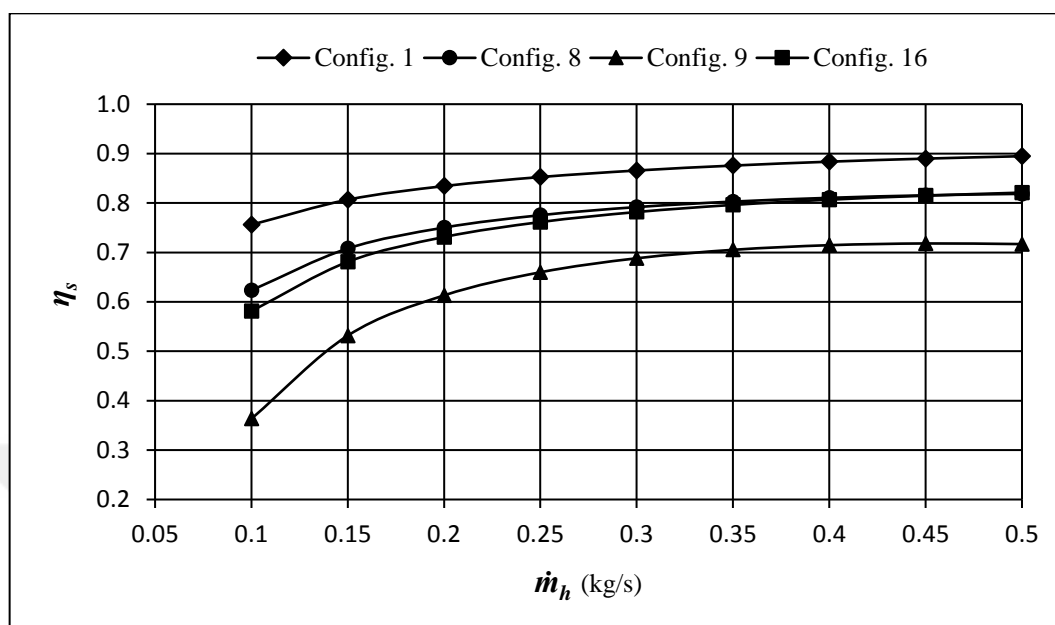


Figure 4.6 The change of second law efficiency with respect to hot side mass flow rate.

This peculiar behavior may be explained with the information provided by Figure 4.5. The decrease in \dot{S}_{gen}/C_{min} (or \dot{S}_{gen}/\dot{m}_h with constant specific heat) is considered to be the reason of the increase in η_s . This means that lower value of normalized entropy generation rate maintains higher second law efficiency and vice versa. On the other hand, this comment cannot be possible without implementation of Figure 4.5 and someone only looking at Figure 4.4 can reach to a different conclusion about the second law efficiency of the given configurations.

4.3 Intercooler and Engine Performance Results

In this part, an engine operating on an air-standard dual cycle with a compression ratio of 16.5 is used. In order to see the effect of intercooling on engine operating conditions, three different cases are studied on this engine. First, engine is considered to be naturally aspirated next, engine is turbocharged but not intercooled and last, engine is turbocharged and intercooled.

For the engine, pressure ratio and cut-off ratio is taken as 1.6 and 1.9, respectively. Also to provide a clear understanding, $P - v$ diagram of the cycle is given in Figure 4.7. Here the aim is to find the temperatures of each thermodynamic state (state 1 to 5) for aforementioned three cases and compare them with each other. Whenever necessary, pressure ratio of the turbocharger compressor is taken as 2.5 and intercooler is considered to provide 60 K temperature drop with 1.5% pressure loss.

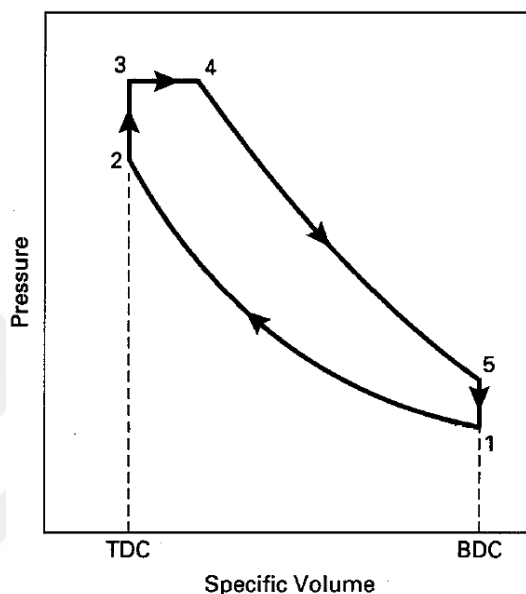


Figure 4.7 $P - v$ diagram of an air-standard dual cycle [Modified from 2].

For three cases, temperatures of all states in the cycle and also the density of the charge air at the inlet to the cylinders are given in Table 4.4.

Table 4.4 Charge air density and temperatures in the cycle for different engine operation types.

Engine operation type	$\rho_{i,air}$ kg/m ³	T_1 K	T_2 K	T_3 K	T_4 K	T_5 K
1. Naturally aspirated.	1.184	298.15	915.02	1464.03	2781.65	1171.68
2. Turbocharged and non-intercooled.	2.279	387.38	1188.85	1902.15	3614.09	1522.32
3. Turbocharged and intercooled.	2.656	327.38	1004.71	1607.53	3054.31	1286.53

As it is seen in the table, when the engine is turbocharged the charge air density increases more than 1.9 times compared to naturally aspirated one. However in this case the temperature throughout the entire cycle is also increased. The peak temperature at the end of the combustion reaches more than 3600 K. This creates high thermal loadings on the engine during operation and also increases heat transfer losses. Such a problem can be diminished by cooling the charge air before entry to the cylinders as in the case of turbocharged and intercooled engines. Also this cooling further increases the density of charge air. As deduced from table, the turbocharged and intercooled engine has nearly 16.6% higher inlet air density when compared with the uncooled one. The peak temperature in the cycle is reduced substantially. Also enhancement in density of air with intercooling provides better volumetric efficiency for the engine and raises the mean effective pressure in the cylinders. These improvements in the engine operating conditions in fact reveal the importance of the intercooling applications in internal combustion engines.

By the way, increasing density allows burning higher amount of fuel, thus more power can be produced in the same engine provided that it mechanically withstands the high pressure and temperature during operation.

At this point it is appropriate to clarify whether utilizing an intercooler in a turbocharged engine is always feasible or not. This statement can be explained by establishing Figure 4.8 in which the effect of intercooling on inlet air density is given for different compressor pressure ratios.

In Figure 4.8 the notation given in Figure 3.1 is used and compression process is considered to be isentropic. The pressure drop in the intercooler is neglected and cooling fluid (ambient air) temperature and pressure are taken as 298.15 K and 101.325 kPa, respectively.

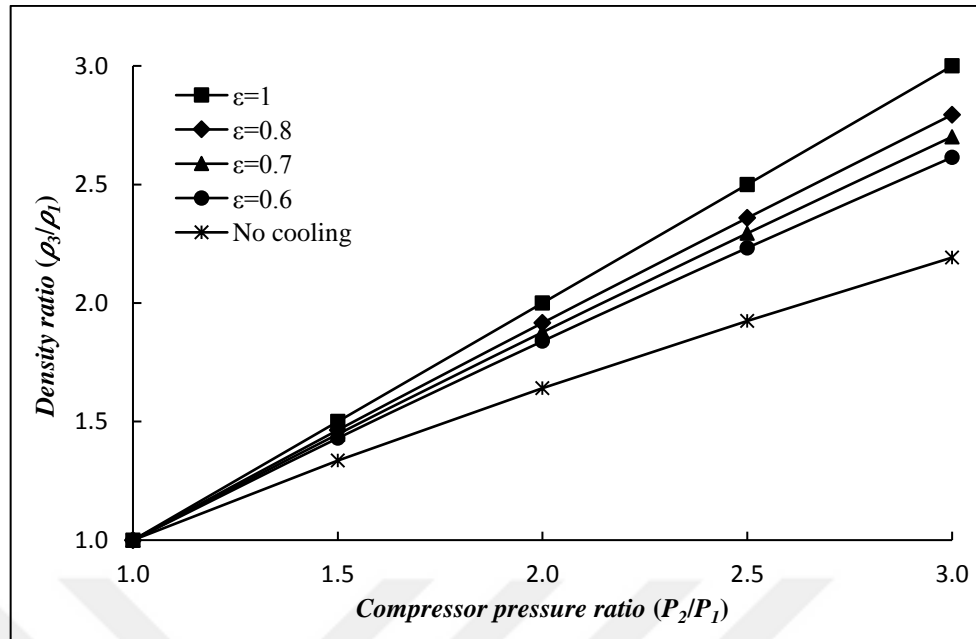


Figure 4.8 Effect of charge cooling on inlet air density.

As seen in Figure 4.8, no cooling and full cooling lines ($\epsilon = 1$) are approaching to each other as the compressor pressure ratio is decreased. It means that at low compression ratios the charge air cooling process does not provide significant density rise, and thus becomes impractical. This is valid especially for compression ratios less than 1.5. On the other hand, for 2.0 and higher compression ratios charge air cooling seems to be inevitable and provides high inlet air density.

Finally, if the effect of pressure drop on the charge air cooling process is investigated, it is understood that losing high amount of pressure during cooling deteriorates the advantages of the process. This effect can better clarified by looking at Figure 4.9 which shows the effect of pressure drop on inlet air density in an intercooler having 80% effectiveness. As the pressure drop increases the benefit of charge air cooling diminishes. It becomes significant especially at high compression ratios and with pressure losses more than 5%.

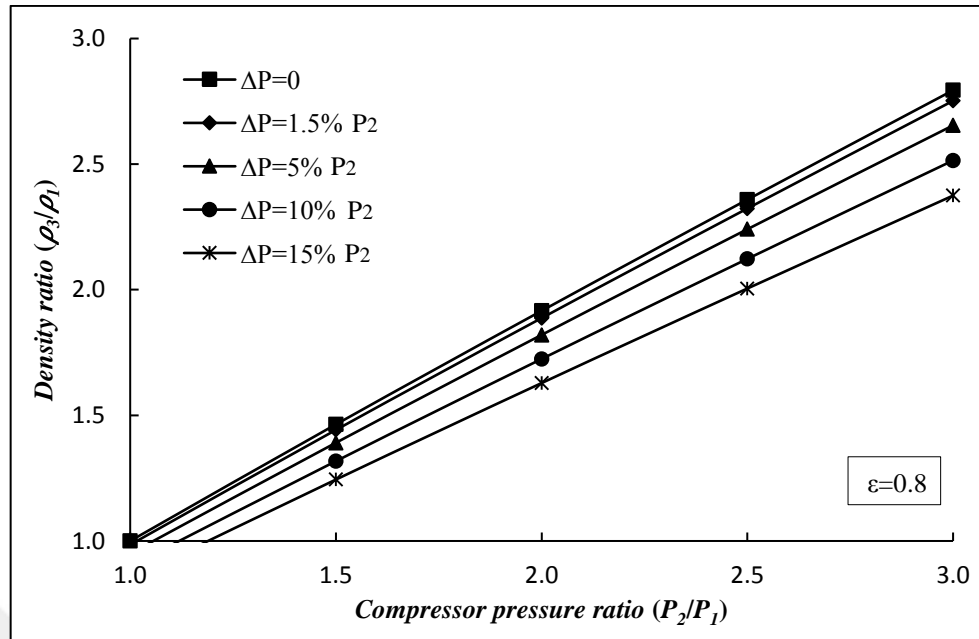


Figure 4.9 Effect of pressure drop on inlet air density.

To sum up, as deduced from last two figures, intercooling application turn into a necessity especially at high compressor pressure ratios and also less than 5% pressure drop should be ensured in the charge air during cooling.

CHAPTER 5

DISCUSSION AND CONCLUSION

In this study, compact plate-fin heat exchangers more specifically intercoolers used in turbocharged engines are theoretically examined. 20 different intercooler configurations housing various fin geometries are established. Sizing and rating procedures are performed on these configurations.

While sizing, operating conditions are taken as the same for all configurations and resulting dimensions of them are compared with each other. While rating, input conditions and dimensions are taken as the same and the resulting performance data is compared with each other in terms of first and second law of thermodynamics. Moreover, the influence of charge air flow rate (hot side mass flow rate) on the performance of the configurations is presented. Effect of intercooling on the engine operating conditions and the feasibility of the intercooling process are discussed.

A computer program is written to handle the iterative solution steps and thus speed up the calculations. During the analysis, the longitudinal heat conduction effects are examined and found to be negligible due to low effectiveness of the intercooler (while sizing) and highly unbalanced flow characteristics of the process. Longitudinal heat conduction effects are not quite serious in heat exchangers having effectiveness values less than 0.9 [8] and also there is no available data for longitudinal heat conduction in the literature for an intercooler application having such an unbalanced flow. This further supports the claim about the negligible effect of it for this study. Furthermore, the pressure drops in the fluids are evaluated such that they only include core pressure drop. The losses in fluid distribution elements are not considered. It is obvious that the overall pressure drop will be higher in the process when losses in inlet and outlet headers are included.

Basically 5 different fin types, namely plain (triangular and rectangular) fin, louvered fin, offset strip fin, wavy fin and perforated fin are proposed for 20 intercooler configurations.

Among these types, offset strip fins provide smaller intercooler volumes than the others for given input and output conditions but their excessive stack heights make their placement on the engine compartment impossible. On the other hand, when the size is preset and thermal-hydraulic performances are investigated, offset strip fins show very good heat transfer performance but also lead to unacceptable amount of pressure drops. Therefore, using offset strip fins, especially on both flow sides, for this particular intercooling application seems to be unreasonable.

Louvered fins do not show as good heat transfer performance as offset strip fins. However they provide more suitable intercooler dimensions and fewer losses in the fluid pressures. This makes their usage more plausible when compared to offset strip fins. Also it should be mentioned that the manufacturing cost of louvered fins are lower than offset strip fins when produced in very large quantities and they allow flexibility in fin spacing due to their triangular cross-sections.

Plain fins are straight fins (i.e. uncut in the flow direction) and thus differ from interrupted fins such as offset strip fins and louvered fins. They generally provide poorer heat transfer performance but better pressure drop characteristics as seen in the results. It is convenient to use these fin types where the allowed pressure drop is low for a fixed frontal area. For an intercooler application mostly their heat transfer performances are adequate and pressure drops are satisfactorily low. Since being less expensive, plain surfaces are more preferable than interrupted ones provided that it can fulfill the given duty. Furthermore, using triangular or rectangular plain fins depends on the requirements. Triangular plain fins are less expensive, can be produced at a faster rate and have improved flexibility of adjustable fin density, however not structurally strong as rectangular ones for the same passage size and fin thickness.

Being uncut but wavy in the flow direction, wavy fins enable better heat transfer coefficients however lead to higher friction factors when compared to plain fins. This situation can be clearly seen from Table 4.2. Both the heat transfer and pressure drop values are larger for wavy fins. In addition to that, because of having high friction factor, limiting pressure drop to low values results in high stack heights in the

intercooler. Wavy fins may not be preferred for such an intercooler application because of these performance characteristics.

Perforated fin surfaces have either round or rectangular perforations. The holes interrupt the flow and may increase heat transfer coefficient. However, considerable amount of heat transfer surface is lost to form these holes. Their heat transfer performances are comparable to wavy fins as seen in the results. Amount of pressure drop is less than wavy fins but again high for an intercooler application.

When it comes to the second law analysis of the surfaces, their second law performances vary depending on the heat transfer and pressure drop characteristics of them. Here the important point is that, it is not possible to eliminate entropy generation or exergy destruction in the intercoolers even with an infinite surface area and zero pressure drops. The reason is the unbalanced flow and it is unavoidable in these configurations. High quality fluid (hot fluid) is transformed into a low quality one during heat transfer, but other fluid (cold fluid) cannot be raised to the same high quality due to its larger mass flow rate. The best way to minimize entropy generation and correspondingly exergy destruction is to decrease pressure losses on both flow sides as much as possible. By doing so, second law efficiency of the process is increased.

Mass flow rate of hot fluid affects the performance and this effect is also investigated for some configurations. Low flow rates correspond to the low speed engine operations and at these speeds intercooler provides better effectiveness and less pressure drops. Increase in mass flow rate however, leads to reduction in effectiveness even if the heat transfer rate is increased. Pressure drop performance is also influenced unfavorably. Next, in terms of second law: nondimensional entropy generation rate decreases and second law efficiency increases with an increase in mass flow rate.

Last, the effect of intercooler on an engine performance is examined and the decrease in engine operating temperatures with the utilization of the intercooler is established. The importance of intercooling process especially at high compressor pressure ratios

(2 or more), are explained with charts. It is also shown that not to diminish benefits of intercooling, the charge air pressure drop should be maintained below 5%.

Finally, it could be convenient to touch on some important considerations related to intercooler surface specifications. While selecting the material for the surface, density and thermal conductivity of it should be taken into consideration. Having low density and high thermal conductivity maintains less weight and good conduction characteristics, respectively. Aluminum is one of the best available material types that can satisfy aforementioned properties and thus mostly preferred in intercooler applications. Despite having remarkable thermal properties, copper may not be preferred due to its high density. On the other hand, a potential fouling or clogging problem due to particulates and moisture can be faced during operation thus; such cases should also be accounted while selecting the fin type.

REFERENCES

- [1] Heywood, J. B., “Internal Combustion Engine Fundamentals”, McGraw-Hill, New York, 1988.
- [2] Pulkrabek, W. W., “Engineering Fundamentals of the Internal Combustion Engines”, Prentice Hall, Upper Saddle River, N. J., 1997.
- [3] Çengel, Y. A. & Boles, M. A., “Thermodynamics: An Engineering Approach”, (5th Ed.), McGraw-Hill, Boston, 2006.
- [4] Bilen, K., “Turbo Doldurmalı Bir Dizel Motoru İçin Ara Soğutucu Dizaynı” M.Sc. Thesis, Kırıkkale University, Graduate School of Natural and Applied Sciences, Kırıkkale-Turkey, 1998.
- [5] Arcoumanis, C., “Internal Combustion Engines”, Academic Press, London, 1988.
- [6] Watson, N. & Janota, M. S., “Turbocharging the Internal Combustion Engine”, Macmillan Press, London, 1982.
- [7] Shah, R. K. & Sekulic, D. P., “Fundamentals of Heat Exchanger Design”, John Wiley and Sons Inc., New Jersey, 2003.
- [8] Kays, W. M. & London, A. L., “Compact Heat Exchangers” (3rd Reprint Ed.), Krieger Publishing Company, Florida, 1988.
- [9] London, A. L. & Shah, R. K., “Offset Rectangular Plate-fin Surfaces-Heat Transfer and Flow Friction Characteristics” ASME J. Eng. Power, 90(3), 218-228, 1968.
- [10] Ismail, L. S. & Ranganayakulu, C. & Shah, R. K., “Numerical Study of Flow Patterns of Compact Plate-fin Heat Exchangers and Generation of Design Data for Offset and Wavy Fins” Int. J. Heat and Mass Transfer, 52(17-18), 3972-3983, 2009.

- [11] Manglik, R. M. & Bergles, A. E., "Heat Transfer and Pressure Drop Correlations for the Rectangular Offset Strip Fin Compact Heat Exchanger" *Experimental Thermal and Fluid Science*, 10(2), 171-180, 1995.
- [12] Kim, M. S. & Lee, J. & Yook, S. J. & Lee, K. S., "Correlations and Optimization of a Heat Exchanger with Offset Strip Fins" *Int. J. Heat and Mass Transfer*, 54(9-10), 2073-2079, 2011.
- [13] Yang, Y. & Li, Y., "General Prediction of the Thermal Hydraulic Performance for Plate-fin Heat Exchanger with Offset Strip Fins" *Int. J. Heat and Mass Transfer*, 78, 860-870, 2014.
- [14] Cowell, T. A. & Heikal, M. R. & Achaichia, A., "Flow and Heat Transfer in Compact Louvered Fin Surfaces" *Experimental Thermal and Fluid Science*, 10(2), 192-199, 1995.
- [15] Ryu, K. & Lee, K. S., "Generalized Heat-Transfer and Fluid-Flow Correlations for Corrugated Louvered Fins" *Int. J. Heat and Mass Transfer*, 83, 604-612, 2015.
- [16] Li, W. & Wang, X., "Heat Transfer and Pressure Drop Correlations for Compact Heat Exchangers with Multi-Region Louver Fins" *Int. J. Heat and Mass Transfer*, 53(15-16), 2955-2962, 2010.
- [17] Vaisi, A. & Esmaeilpour, M. & Taherian, H., "Experimental Investigation of Geometry Effects on the Performance of A Compact Louvered Heat Exchanger" *Applied Thermal Engineering*, 31(16), 3337-3346, 2011.
- [18] Ranganayakulu, C. & Seetharamu, K. N. & Sreevatsan, K. V., "The Effect of Longitudinal Heat Conduction in Compact Plate-fin and Tube-fin Heat Exchangers Using a Finite Element Method" *Int. J. Heat and Mass Transfer*, 40(6), 1261-1277, 1997.

- [19] Ranganayakulu, C. & Seetharamu, K. N., “The Combined Effects of Wall Longitudinal Heat Conduction, Inlet Fluid Flow Nonuniformity and Temperature Nonuniformity in Compact Tube-fin Heat Exchangers: a Finite Element Method” *Int. J. Heat and Mass Transfer*, 42(2), 263-273, 1999.
- [20] Shah, R. K. & Skiepko, T., “Entropy Generation Extrema and Their Relationship with Heat Exchanger Effectiveness-Number of Transfer Unit Behavior for Complex Flow Arrangements” *ASME J. Heat Transfer*, 126(6), 994-1002, 2005.
- [21] Gheorghian, A. T. & Dobrovicescu, A. & Popescu, L. G. & Cruceru, M. & Diaconu, B. M., “Entropy Generation Assessment Criterion for Compact Heat Transfer Surfaces” *Applied Thermal Engineering*, 87, 137-149, 2015.
- [22] Canlı, E. & Darıcı, S. & Doğan, S. & Özgören, M., “Kompakt Isı Değiştiricilerinde Kararlı Çalışma Halindeki Ekserji Yıkımının Deneysel Olarak Tespiti ve Aynı Isıl Kapasite Oranı için Üç Farklı Isı Değiştiricisinin Ekserji Yıkımlarının Karşılaştırılması” 11. Ulusal Tesisat Mühendisliği Kongresi, 17-20 Nisan 2013, MMO Tepekule Kongre ve Sergi Merkezi-İzmir: TMMOB Makina Mühendisleri Odası, 1149-1175, 2013.
- [23] Çengel, Y. A. & Ghajar, A. J., “Heat and Mass Transfer: Fundamentals and Applications” (4th Ed.), McGraw-Hill, New York, 2011, p. 652.
- [24] Incropera, F. P. & Dewitt, D. P. & Bergman, T. L. & Lavine, A. S., “Fundamentals of Heat and Mass Transfer” (6th Ed.), John Wiley & Sons Inc., New Jersey, 2007.
- [25] Mills, A. F., “Heat Transfer” (2nd Ed.), Prentice Hall, Upper Saddle River, N. J., 1999.
- [26] Bejan, A., “Entropy Generation Minimization”, CRC Press LLC, Florida, 1995, p. 23.

- [27] Bejan, A., "The Concept of Irreversibility in Heat Exchanger Design: Counterflow Heat Exchangers for Gas-to-Gas Applications" *ASME J. Heat Transfer*, 99(3), 374-380, 1977.
- [28] Bejan, A., "Advanced Engineering Thermodynamics", John Wiley and Sons Inc., New Jersey, 2006, p. 589.
- [29] Hesselgreaves, J. E., "Rationalisation of Second Law Analysis of Heat Exchangers" *Int. J. Heat and Mass Transfer*, 43(22), 4189-4204, 2000.
- [30] Zimparov V. & Vulchanov, N. L., "Performance Evaluation Criteria for Enhanced Heat Transfer Surfaces" *Int. J. Heat and Mass Transfer*, 37(12) 1807-1816, 1994.
- [31] Prasad, R. C. & Shen, J., "Performance Evaluation of Convective Heat Transfer Enhancement Devices Using Exergy Analysis" *Int. J. Heat and Mass Transfer*, 36(17), 4193-4197, 1993.
- [32] Bruges, E. A., "Available Energy and the Second Law Analysis", Academic Press Inc., London, 1959.
- [33] Yılmaz, M. & Sara, O. N. & Karşı, S., "Performance Evaluation Criteria for Heat Exchangers Based on Second Law Analysis" *Exergy Int. J.*, 1(4), 278-294, 2001.

APPENDICES

Appendix A: Surface Characteristics of Fins.

Appendix B: j and f Factor Equations and Reynolds Number Ranges.

Appendix C: Thermophysical Properties of Air.

Appendix D: K_c and K_e Coefficients.



Appendix A – Surface Characteristics of Fins

Table A.1 Surface characteristics of fins [8].

Fin type	Fin density m^{-1}	Plate spacing b mm	Hydraulic diameter D_h mm	Fin thickness δ_f mm	Surface area density β m^2/m^3	Fin area / Total area A_f/A m^2/m^2
Plain 9.03	355.5	20.9	4.463	0.203	800.5	0.888
Plain 11.11	437	6.35	3.081	0.152	1204	0.756
Plain 19.86	782	6.35	1.875	0.152	1841	0.849
Plain 12.00T	472	6.35	2.870	0.152	1288	0.733
Louvered 1/2-6.06	239	6.35	4.453	0.152	840	0.640
Louvered 3/8(a)-8.7	343	6.35	3.650	0.152	1007	0.705
Louvered 1/4-11.1	437	6.35	3.084	0.152	1204	0.756
Louvered 3/4-11.1	437	6.35	3.084	0.152	1204	0.756
Offset strip 1/8-15.61	615	6.35	2.380	0.102	1548	0.809
Offset strip 1/8-19.86	782	2.49	1.540	0.102	2254	0.785
Offset strip 1/9-24.12	950	1.91	1.209	0.102	2830	0.665
Offset strip 1/10-19.74	777	1.29	1.219	0.051	3028	0.508
Wavy 11.5-3/8W	453	9.25	3.023	0.254	1138	0.822
Wavy 17.8-3/8W	701	10.49	2.123	0.152	1686	0.892
Perforated 13.95P	510	5.08	2.504	0.305	1250	0.705

Appendix B – j and f Factor Equations and Reynolds Number Ranges

Table B.1 j factor equations for fin types.

Fin type Equation type	$j_1 = a_j + \frac{b_j}{\ln Re} + \frac{c_j}{(\ln Re)^2} + \frac{d_j}{(\ln Re)^3}$ $j_2 = \frac{a_j + \frac{c_j}{\ln Re} + \frac{e_j}{(\ln Re)^2} + \frac{g_j}{(\ln Re)^3}}{1 + \frac{b_j}{\ln Re} + \frac{d_j}{(\ln Re)^2} + \frac{f_j}{(\ln Re)^3}}$						
	a_j	b_j	c_j	d_j	e_j	f_j	g_j
Plain 9.03 j_2	$-76 \cdot 10^{-5}$	-0.4364	$77 \cdot 10^{-6}$	0.06265	$18 \cdot 10^{-6}$	-0.00297	$2 \cdot 10^{-6}$
Plain 11.11 j_2	$-34 \cdot 10^{-4}$	-0.4894	$97 \cdot 10^{-5}$	0.07797	$-75 \cdot 10^{-6}$	-0.0041	$69 \cdot 10^{-8}$
Plain 19.86 j_2	$-33 \cdot 10^{-4}$	-0.4955	$93 \cdot 10^{-5}$	0.08017	$-67 \cdot 10^{-6}$	-0.0043	$11 \cdot 10^{-8}$
Plain 12.00T j_2	-0.0149	-0.5373	0.00505	0.08904	-0.00056	-0.00476	$2 \cdot 10^{-5}$
Louvered 1/2-6.06 j_2	-0.0117	-0.5071	0.00332	0.07946	-0.00029	-0.00399	$66 \cdot 10^{-7}$
Louvered 3/8(a)-8.7 j_1	-0.0494	1.0440	-6.9121	18.199	-	-	-
Louvered 1/4-11.1 j_2	-0.0268	-0.6097	0.00927	0.11338	-0.0010	-0.00668	$33 \cdot 10^{-6}$
Louvered 3/4-11.1 j_2	-0.0077	-0.4720	0.00219	0.07045	-0.00019	-0.0034	$48 \cdot 10^{-7}$
Offset strip 1/8-15.61 j_1	-0.0192	0.56408	-5.2580	20.6722	-	-	-
Offset strip 1/8-19.86 j_1	-0.0505	1.13017	-8.2922	24.2204	-	-	-
Offset strip 1/9-24.12 j_1	-0.1099	2.49627	-18.266	47.1236	-	-	-
Offset strip 1/10-19.74 j_1	0.02304	-0.2802	0.77926	3.82960	-	-	-
Wavy 11.5-3/8W j_1	0.04332	-1.2929	12.3976	-33.041	-	-	-
Wavy 17.8-3/8W j_1	$-33 \cdot 10^{-5}$	-0.1300	2.00937	-3.3043	-	-	-
Perforated 13.95P j_2	-0.0051	-0.4705	0.00134	0.07123	$94 \cdot 10^{-6}$	-0.0035	$70 \cdot 10^{-8}$

Table B.2 f factor equations for fin types.

Fin type Equation type	$f_1 = a_f + \frac{b_f}{\ln Re} + \frac{c_f}{(\ln Re)^2} + \frac{d_f}{(\ln Re)^3}$ $f_2 = \frac{a_f + \frac{c_f}{\ln Re} + \frac{e_f}{(\ln Re)^2} + \frac{g_f}{(\ln Re)^3}}{1 + \frac{b_f}{\ln Re} + \frac{d_f}{(\ln Re)^2} + \frac{f_f}{(\ln Re)^3}}$						
	a_f	b_f	c_f	d_f	e_f	f_f	g_f
Plain 9.03 f_2	-0.0047	-0.4324	0.00113	0.06164	$-58 \cdot 10^{-6}$	-0.0029	$-12 \cdot 10^{-7}$
Plain 11.11 f_1	-0.2554	6.79693	-59.194	175.071	-	-	-
Plain 19.86 f_2	-0.0026	-0.4926	0.00014	0.08060	0.00012	-0.00441	$-13 \cdot 10^{-6}$
Plain 12.00T f_2	-0.0803	-0.5390	0.02823	0.09122	-0.00329	-0.00512	$125 \cdot 10^{-6}$
Louvered 1/2-6.06 f_1	-0.2944	8.04565	-69.099	207.316	-	-	-
Louvered 3/8(a)-8.7 f_1	-0.5694	14.1419	-113.16	315.009	-	-	-
Louvered 1/4-11.1 f_1	-0.2354	5.93173	-48.212	147.457	-	-	-
Louvered 3/4-11.1 f_1	0.11827	-1.7682	5.25793	21.2135	-	-	-
Offset strip 1/8-15.61 f_1	-0.0770	3.81759	-43.582	162.977	-	-	-
Offset strip 1/8-19.86 f_1	0.06376	0.12183	-12.703	76.8808	-	-	-
Offset strip 1/9-24.12 f_1	0.25156	-3.3547	10.2473	22.7856	-	-	-
Offset strip 1/10-19.74 f_1	0.20398	-2.3488	3.0778	38.7971	-	-	-
Wavy 11.5-3/8W f_1	0.55293	-13.255	104.425	-243.271	-	-	-
Wavy 17.8-3/8W f_1	0.14368	-3.1185	21.8327	-30.328	-	-	-
Perforated 13.95P f_2	-0.0125	-0.4729	0.00353	0.07295	$-28 \cdot 10^{-5}$	-0.0037	$336 \cdot 10^{-8}$

Table B.3 Reynolds number ranges for j and f factor equations [8].

Fin type	Reynolds number range
Plain 9.03	$800 < Re < 15000$
Plain 11.11	$500 < Re < 10000$
Plain 19.86	$400 < Re < 8000$
Plain 12.00T	$200 < Re < 8000$
Louvered 1/2-6.06	$600 < Re < 10000$
Louvered 3/8(a)-8.7	$500 < Re < 8000$
Louvered 1/4-11.1	$500 < Re < 8000$
Louvered 3/4-11.1	$500 < Re < 10000$
Offset strip 1/8-15.61	$300 < Re < 6000$
Offset strip 1/8-19.86	$300 < Re < 4000$
Offset strip 1/9-24.12	$300 < Re < 2000$
Offset strip 1/10-19.74	$300 < Re < 3000$
Wavy 11.5-3/8W	$400 < Re < 10000$
Wavy 17.8-3/8W	$600 < Re < 5000$
Perforated 13.95P	$500 < Re < 10000$

Appendix C – Thermophysical Properties of Air

Table C.1 Thermophysical properties of air at one atmospheric pressure [Modified from 24].

Temperature K	c_p kJ/(kg·K)	$\mu \cdot 10^7$ N·s/m ²	$k \cdot 10^3$ W/(m·K)	Pr
100	1.032	71.1	9.34	0.786
150	1.012	103.4	13.8	0.758
200	1.007	132.5	18.1	0.737
250	1.006	159.6	22.3	0.720
300	1.007	184.6	26.3	0.707
350	1.009	208.2	30.0	0.700
400	1.014	230.1	33.8	0.690
450	1.021	250.7	37.3	0.686
500	1.030	270.1	40.7	0.684
550	1.040	288.4	43.9	0.683
600	1.051	305.8	46.9	0.685
650	1.063	322.5	49.7	0.690
750	1.087	354.6	54.9	0.702
800	1.099	369.8	57.3	0.709
850	1.110	384.3	59.6	0.716
900	1.121	398.1	62.0	0.720
950	1.131	411.3	64.3	0.723
1000	1.141	424.4	66.7	0.726
1100	1.159	449.0	71.5	0.728
1200	1.175	473.0	76.3	0.728
1300	1.189	496.0	82.0	0.719
1400	1.207	530.0	91.0	0.703
1500	1.230	557.0	100.0	0.685

Appendix D – K_c and K_e Coefficients

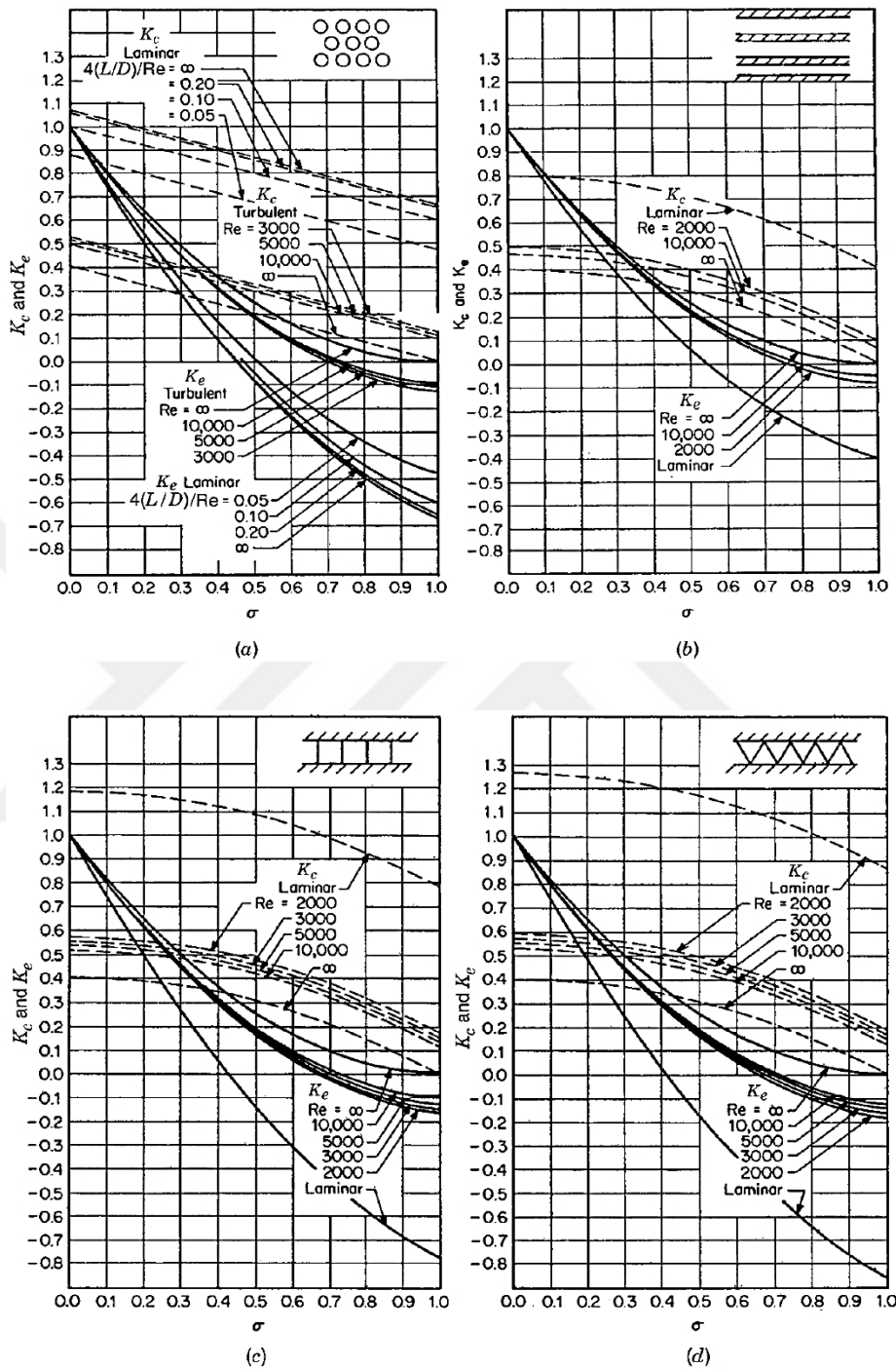


Figure D.1 Entrance and exit pressure loss coefficients for (a) a multiple circular tube core, (b) multiple-tube flat-tube core, (c) multiple square tube core, and (d) multiple triangular tube core with abrupt contraction (entrance) and abrupt expansion (exit) [7].

CURRICULUM VITAE

PERSONAL INFORMATION

Name Surname : Ahmet Yasin SEDEF
Date of Birth : 1989
Phone : +90 506 5717438
E-mail : aysedef@ybu.edu.tr



EDUCATION

High School : Ümitkoy Anatolian High School / ANKARA (2003-2007)
(82.75/100)
Bachelor : University of Gaziantep / GAZİANTEP (2008-2013)
(3.61/4.0)
Master Degree : Ankara Yıldırım Beyazıt University / (2014-continued)

WORK EXPERIENCE

Research Assist.: Ankara Yıldırım Beyazıt University / (2014-continued)

TOPICS OF INTEREST

- Thermodynamics
- Heat Transfer
- Fluid Mechanics
- Internal Combustion Engines